

Santa Clara University

Scholar Commons

Bioengineering Senior Theses

Engineering Senior Theses

6-2021

MilkGuard: Predictive Modeling and Mobile App Development for Affordable, Usable Breast Milk Diagnostic

Beau Hsia

Emma McCurry

Follow this and additional works at: https://scholarcommons.scu.edu/bioe_senior



Part of the [Biomedical Engineering and Bioengineering Commons](#)

SANTA CLARA UNIVERSITY

Department of Bioengineering

I HEREBY RECOMMEND THAT THE THESIS PREPARED UNDER MY
SUPERVISION BY

Beau Hsia, Emma McCurry

ENTITLED

MILKGUARD: PREDICTIVE MODELING AND MOBILE APP
DEVELOPMENT FOR AFFORDABLE, USABLE BREAST MILK
DIAGNOSTIC

BE ACCEPTED IN PARTIAL FULFILLMENT OF THE REQUIREMENTS FOR THE DEGREE OF

**BACHELOR OF SCIENCE
IN
BIOENGINEERING**



6/10/2021

Thesis Advisor

Date

M. Mobed-Miremadi

6/10/2021

Thesis Advisor

Date



6/10/2021

Department Chair

Date

**MilkGuard: Predictive Modeling and Mobile App
Development for Affordable, Usable Breast Milk
Diagnostic**

By Beau Hsia and Emma McCurry

SENIOR DESIGN PROJECT REPORT

Submitted to the Department of Bioengineering

of

SANTA CLARA UNIVERSITY

in Partial Fulfillment of the Requirements for the
degree of Bachelor of Science in Bioengineering

Santa Clara, California

2021

Abstract

Breast milk is considered the gold standard of infant nutrition, but some infants around the world lack access to it due to maternal health complications or other considerations. Human breast milk banks do exist to try to alleviate this problem, but most are underfunded and have high operational costs, making it difficult for some infants to obtain safe, reliable donated breast milk.

Existing methods of testing breast milk are expensive, so the MilkGuard project was conceptualized in 2017 as a fast, economical, and highly usable bacterial contamination detection system. Prior to this year, previous MilkGuard teams had developed a system that was faster and more affordable than prior methods, but its main drawbacks were that it was difficult to use and that it lacked the sensitivity to detect low *Escherichia coli* (*E. coli*) contamination levels. To ameliorate these drawbacks, our goals for this year were 1) to improve MilkGuard's sensitivity to the Human Milk Banking Association of North America's (HMBANA) lower limit of detection standard of 10^4 CFU/mL, 2) to increase the ease of the assay process, and 3) to achieve these objectives in an economical and environmentally-friendly way.

Through COMSOL Multiphysics software simulations, we proved the possibility of realistically optimizing biosensor parameters on a computer. Since the simulations were virtual, we discovered an optimal biosensor configuration without the need to purchase, manufacture, and test hundreds of physical sensors. Future teams can quickly confirm these results by building a physical sensor in the lab. We also developed the MilkGuard app, which greatly simplifies the colorimetric analysis process for the user. This mobile app uses our improved color-analysis algorithm which improves detection sensitivity around the HMBANA's lowered limit of detection standard, given the same image data to analyze. The efficacy of our new color analysis algorithm can be confirmed by future teams in the lab, and our current regression curve can be made more robust with a larger sample size.

Taken together, our developments this year have increased the usability and sensitivity of the MilkGuard system, which can improve bacterial contamination testing by milk banks and move one step closer to equitable access to safe breast milk for infants around the world.

Key Words: [milk bank], [breast milk], [infant health], [infant safety], [bacteriological testing], [*E. coli* detection], [hydrogel biosensor], [alginate hydrogel]

Acknowledgements

Our deepest gratitude goes to Dr. Ashley Kim and Dr. Maryam Mobed-Miremadi, our advisors for this project. Our work would not have been possible without their invaluable support throughout every step of this process.

This project could not have been realized without Santa Clara University's Frugal Innovation Hub, which has sponsored the MilkGuard project since its conception. Thank you to Frugal Innovation Hub collaborator Gregory Theyel for his feedback on our project.

Thank you to Santa Clara University School of Engineering and Bioengineering Department for your support, and to previous MilkGuard senior design teams and researchers for your efforts. Our work would certainly not have been possible without you.

We thank Santa Clara University for providing us with a holistic education, and for rooting its educational mission in a vision to build a more competent, conscious, and compassionate world.

Thank you to our family, friends, and supporters who have helped us through the failures and successes of this project, and who helped us maintain sanity throughout the remote work required during the COVID-19 pandemic.

And finally, we give thanks to Mother's Milk Bank of San José for their collaboration in the early stages of the MilkGuard project. Our work is dedicated to milk banks nationally and worldwide, and to the mothers and infants they aim to serve— especially those who are currently unable to acquire safe and affordable donated human breast milk. Milk banks: thank you for dedicating your time, resources, and careers to increasing access to breast milk. Mothers: we are in awe of your continued perseverance and dedication to your children. We stand with you and pray that our work would benefit you.

Table of Contents

List of Figures	8
List of Tables	9
Chapter 1: Introduction	10
1.1 Importance of Breast Milk	10
1.2 Lack of Access to Breast Milk	10
1.3 Milk Bank Operation and Challenges	10
1.4 The MilkGuard Solution	11
Chapter 2: Review of Field	12
2.1 Current Solutions for Bacteriological Testing	12
2.2 Literature Review	13
Chapter 3: Previous Achievements & Current Challenges	14
3.1 Colorimetric Reaction	14
3.2 Alginate Hydrogel	14
3.3 Biosensor Geometry	15
3.4 Colorimetric Analysis	15
3.5 Image Analysis Challenges	15
3.6 Lower Limit of Detection Challenges	17
3.7 Rationale for Current Work	17
Chapter 4: Materials & Methods	18
4.1 MilkGuard Subsystems	18
4.2 Simulation Materials	18
4.2.1 Chemical & Biological Reagents	18
4.2.2 COMSOL Multiphysics	18
4.2 Simulation Methods	19
4.2.1 Laboratory Methods	19
4.2.2 Simulation Geometry	19
4.2.3 Simulation Parameters	19
4.2.4 Geometry Optimization	22
4.4 Mobile App Materials	24
4.5 Mobile App Methods (long section)	25
4.5.1 RGB Color Balance	25
4.5.2 Conversion to HSL Color Space	25
4.5.3 HSL Distance	28
Chapter 5: Results	29

5.1 Simulation Outcomes	29
5.1.1 Comparison to Experimental Results	29
5.1.2 Geometry Optimization	30
5.1.3 Future Work	32
5.2 Color Analysis / Mobile App Results	33
Chapter 6: Discussion and Recommendations	37
6.1 Biosensor Simulation & Optimization	37
6.2 Mobile App & Color Analysis Algorithm	37
6.3 Cost Considerations	40
6.4 Next Steps	40
6.4.1 Remaining Challenges	40
6.4.2 Immediate Next Steps	41
6.4.3 Long Term Next Steps	42
Chapter 7: Ethics and Engineering Standards	43
7.1 Ethical Justification	43
7.2 Engineering Standards	44
7.2.3 Health & safety	44
7.2.4 Usability	45
7.2.5 Environmental impact	45
7.2.6 Social	45
Chapter 8: Conclusions	47
Chapter 9: References	48
Chapter 10: Appendix	55
10.1 Team Members and Roles	55
10.2 Key Acronyms and Abbreviations	55

List of Figures

- Figure 1.** Reaction schematic for X-gal hydrolysis in the presence of β -galactosidase.
- Figure 2.** Colorimetric ladders generated by previous teams to compare sensor sensitivity.
- Figure 3.** Graphs depicting the calculated RGB ratio for various concentrations of *E. coli* induced with DHBM and whole bovine milk.
- Figure 4.** Effectiveness constant as a function of capsule radius, from experimentally derived values.
- Figure 5.** An HSL color cylinder model showing the corresponding dimensions for Hue, Saturation, and Lightness.
- Figure 6.** Comparison of experimental data and COMSOL model surface concentration outputs for blue reaction precipitate.
- Figure 7.** Reaction precipitates concentration in milk samples (i.e. outside of the biosensor capsule) as a function of capsule radius at selected time indices.
- Figure 8.** Reaction precipitate concentration over time for capsules of selected radii.
- Figure 9.** Induced blue color represented on the HSL color space cylinder model.
- Figure 10.** Graphs depicting the calculated Color Distance Values for various concentrations of *E. coli* induced with DHBM and whole bovine milk.
- Figure 11.** Graph depicting the calculated Color Distance Value for various concentrations of *E. coli* induced with DHBM in clear wellplates.
- Figure 12.** Diagram showing screenshots from the MilkGuard app.
- Figure 13.** Graphs depicting the calculated color values for various concentrations of *E. coli* before and after application of new algorithm
- Figure 14.** Graphs depicting the calculated color values for various concentrations of *E. coli* induced with DHBM in clear wellplates before and after applying color balance, HSL conversion, and color-distance regression.

List of Tables

- Table 1.** Simulation inputs for COMSOL biosensor model.
- Table 2.** Variable inputs for COMSOL geometry optimization.

Chapter 1: Introduction

1.1 Importance of Breast Milk

Breast milk is considered the gold standard of infant nutrition worldwide [1]. Breast milk provides infants with nutrients and energy needed during their early life, and contains antibodies that help guard against common childhood illnesses [3]. Breastfeeding has been linked to enhanced cognitive development and decreased infant mortality. However, access to breast milk remains a challenge for many mothers and babies worldwide. The World Health Organization estimates that 820,000 children around the world could have been saved if optimally breastfed [4].

1.2 Lack of Access to Breast Milk

Some mothers are advised against, or unable to breastfeed. This includes women infected with HIV or human T-lymphotropic virus (type I or type II). Women taking HIV medication or cancer chemotherapy agents should also avoid breastfeeding their infant. Other conditions, such as diabetes and thyroid conditions make it challenging for women to produce or pump enough milk for their infants [5]. This challenge has led to the emergence of breast milk banks worldwide that aim to provide mothers and infants with sufficient, reliable, and safe access to donated human breast milk (DHBM).

1.3 Milk Bank Operation and Challenges

To ensure infant safety, milk banks should maintain rigorous pasteurization and bacteriological testing procedures [4]. The Human Milk Banking Association of North America's (HMBANA) standards requires that a milk bank's medical director, staff, and board of directors include healthcare professionals. All staff must have food safety, food processing, Preventive Controls Qualified Individual (PCQI) training, and must participate in continuing education. Breast milk donors must be screened verbally for (at minimum) HIV-1 and -2, HTLV-1 and -2, hepatitis C, hepatitis B, and syphilis and must be instructed on safe expression techniques. DHBM is accepted only if it was been expressed in the previous 36 hours or was placed in a freezer within 36 hours of expression. All milk banks should follow applicable safety and

quality-assurance processing procedures as defined by the Current Good Manufacturing Practice, FDA, and other governing bodies. Milk banks maintain calibrated pasteurizers, freezers, refrigerators, dish machines, and thermometers. Upon receiving milk from a donor, the donation is recorded, thawed (if necessary), pooled, and mixed under aseptic technique. Pooled DHBM is then strained with a food-grade filter and stored in food-grade plastic bottles. Each bottle is pasteurized at 62.5°C for 30 minutes then rapidly chilled. At this point, one bottle from each batch must be sent to an external lab for bacteriological testing. The remainder of the batch must be placed under refrigeration while awaiting test results. Once the bottle sent for testing passes, the entire batch can be distributed to mothers and infants [6].

The rigorous bacteriological testing procedures makes the DHBM at milk banks safer than the milk purchased from internet sources or from informal exchanges [7]. However, bacteriological testing is also expensive (\$35-81 plus additional labor costs to test 100-200 oz of DHBM [8]) and time consuming [9]. These high costs limit infant access to breast milk [2].

1.4 The MilkGuard Solution

To address current shortcomings and improve infant health through enhanced access to optimal nutrition (human breast milk), MilkGuard has developed a biodegradable, alginate hydrogel biosensor that colorimetrically detects the presence of *Escherichia coli* (*E. coli*) in DHBM [3]. The goal of the MilkGuard biosensor and associated analysis is to create a safe, reliable, affordable, environmentally-friendly, and intuitive way for milk banks to perform bacteriological testing on donated human breast milk within their facilities. In-house testing with an affordable product that does not require lab-access will cut the cost of milk bank operation and therefore reduce the price tag that is currently placed on the safest, most reliable option for mothers who are unable to breastfeed their infants.

Chapter 2: Review of Field

2.1 Current Solutions for Bacteriological Testing

Currently, few available options for the bacteriological testing of breast milk. In addition to the standard bacteriological testing regiment at external laboratory facilities, there are two commercially available testing products. These are discussed below.

Lactation Labs offers a breast milk analysis service for lactating mothers. Lactation Labs markets their product to mothers as a convenient way to analyze the nutritional content of their milk from home. A mother receives a Lactation Labs sample collection kit at home. She then uses the kit to collect a sample of her milk. This sample is then shipped back to Lactation Labs where it is analyzed in a laboratory. Once lab tests are completed and results are compiled, the mother receives a full report of her analysis in her email inbox. Results are typically available in 1–3 weeks, depending on the type of test ordered. Kits are available in basic, standard, and premium options, and cost between \$99 and \$349. While this model of testing is novel for its direct involvement with mothers, Lactation Labs does not currently offer bacteriological testing [4].

My Milk Lab *Mylee* is known for its electrochemical breast milk sensor. Released to market in 2019, Mylee analyzes the composition of HBM and uploads this information to a mobile application. The device uses a few drops of breast milk to analyze the electrochemical properties of the mother's milk. These properties are correlated to existing HBM nutritional data, gathered and generated by Mylee. Results of the analysis are posted to the Mylee mobile application for the mother to view. The Mylee microdevices cost \$349 each, but can be reused by a mother repeatedly. The device does not currently offer bacteriological testing of breast milk. However, My Milk Lab *does* offer separate breast milk bacteriological testing kits. The process of breast milk collection and analysis for these testing kits is similar to that of Lactation Lab's model. The testing of the sample is conducted at an external lab facility at a rate of \$249 per sample [5].

2.2 Literature Review

Biosensor computer-aided design (CAD) modeling has been previously used in bacterial detection applications, such as COMSOL Multiphysics modeling of graphene field-effect transistor biosensors for bacterial detection [6], electrochemical impedance spectroscopy detection for polarizable bacteria [7], and bioluminescent sensors for both *Aliivibrio fischeri* [8] and foodborne bacterial ATP [9]. COMSOL models have also been used to explore the optimal geometry of microfluidic biosensors for detecting food-borne salmonella [10] and interdigitated electrode sensors [11], which can be used for detection of *S. aureus* [12] and *E. coli* [13].

General colorimetric analysis methods have applications in food safety [14], specifically of dairy products [15]; point-of-care diagnostics [16] such as the diagnosis of kidney failure from levels of creatinine [17]; and environmental monitoring [18]. Biomedical applications of smartphone-based technologies include rapid blood hemocytometry and analysis [19-21], parasite detection [22], histological classification [23], skin tumor diagnostics [24], ophthalmology [25], hepatology [26], and other global health applications [27]. Biomedical smartphone applications specifically using colorimetry include ones for methamphetamine [28] or salivary glucose detection. Smartphone applications also exist that test for milk tetracycline residues [29] or hormone levels in milk [30].

Chapter 3: Previous Achievements & Current Challenges

Challenges

3.1 Colorimetric Reaction

The MilkGuard biosensor is an alginate-based hydrogel biosensor with encapsulated 5-bromo-4-chloro-3-indolyl- β -D-galactopyranoside (x-gal). In low glucose, high-lactose environments like DHBM, *E. coli* produces β -galactosidase for the hydrolysis of lactose.. β -galactosidase will also hydrolyze X-gal. The product of the X-gal hydrolysis spontaneously dimerizes into an intense, visible blue precipitate that can be used for colorimetric analyses [See Figure 1].

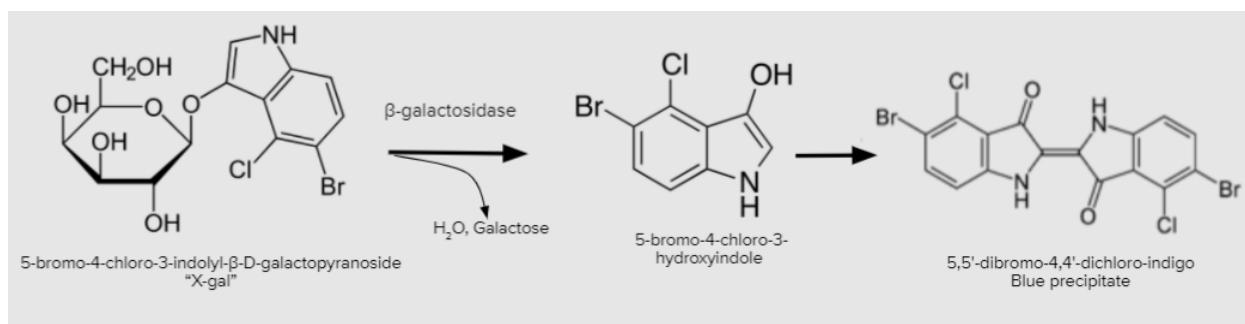


Figure 1: Reaction schematic for X-gal hydrolysis in the presence of β -galactosidase. The blue precipitate product is used in our assay for colorimetric analysis.

The reaction between β -galactosidase and X-gal is usually used in blue-white colony screening in recombinant DNA techniques, but previous MilkGuard teams chose to use this reaction to develop a colorimetric assay to detect the presence of E Coli in breast milk. If present in a donated milk sample, *E. coli* will produce beta galactosidase, which in turn hydrolyzes X-gal and produces a visible blue precipitate that can be quantified.

3.2 Alginate Hydrogel

Previous teams developed a cost-effective, biodegradable alginate hydrogel biosensor for the MilkGuard system. The hydrogel microcapsules are fabricated with a autoclaved 3% (w/v)

solution of alginate and 0.9% (w/v) NaCl as a solvent. Previous observation indicates that sterilization of the alginate materials is necessary to eliminate yeast contamination that produces false positive results [3]. After sterilization and mixing, 1 mL aliquots of the alginate solution are spiked with X-gal. The concentration of X-gal has varied throughout the history of MilkGuard and will need to be finalized in future work. The solution is then stirred and extruded through a standard 304 SS 18 gauge needle based on principles of ionotropic gelation [31]. The microcapsules are dropped into a CaCl₂ solution to facilitate cross linking and washed after 30 minutes of incubation with an NaCl solution.

3.3 Biosensor Geometry

The MilkGuard biosensors were originally paper-based. The porous, filter-paper sensor with reagents deposited onto its surface is an extremely low-cost model [32]. However, alginate hydrogel is much easier to manufacture and uniformly produce. Alginate hydrogel is also extremely low-cost, biodegradable, and can be mixed with X-gal before extrusion [33]. Once alginate hydrogel was selected as the sensor material, ionotropic gelation-based extrusion emerged as the most cost-effective and easily manufacturable mechanism for producing the biosensor. This project, in part, focuses on optimizing the size of spherical capsules produced through ionotropic gelation.

3.4 Colorimetric Analysis

Previous teams obtained colorimetric images using mobile phone photography and analyzed these images using ImageJ computer software. ImageJ returns RGB (red, green, blue) values of selected pixels in an image. Several pixels from each well plate were averaged and analyzed. The blueness index was calculated as “the ratio between the B value for each well and the average of the G and R values.”

3.5 Image Analysis Challenges

After struggling with consistent image analysis due to background lighting changes, previous teams developed a custom-built photography lightbox to minimize the effects of outside light. The lightbox is constructed from black acrylic sheets, with an aperture at the top of the box for a smartphone camera and an LED light unit inside the lightbox to illuminate the sample [34].

Although the custom-built lightbox considerably improved the consistency of the lighting in the images captured for colorimetric analysis, the existing method for image analysis was still unable to differentiate between lower concentrations of bacterial contamination. Figure 3 shows the correlation between color intensity (“blueness”) and bacterial concentration using the imaging methods described above. Notice that 10^4 and 10^5 CFU/mL color intensity values were statistically indistinguishable.



Figure 2: Colorimetric ladders generated by previous teams to compare sensor sensitivity. Varying concentrations of *E. coli* were induced with (a) DHBM and (b) whole bovine milk. We also used these same images to test our colorimetric algorithm.

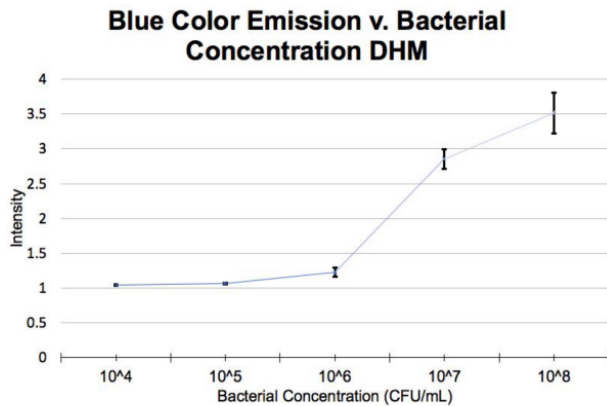


Figure 21. Graph depicting the calculated RGB ratio for different concentrations of *E. coli* induced with donated human breast milk.

(a)

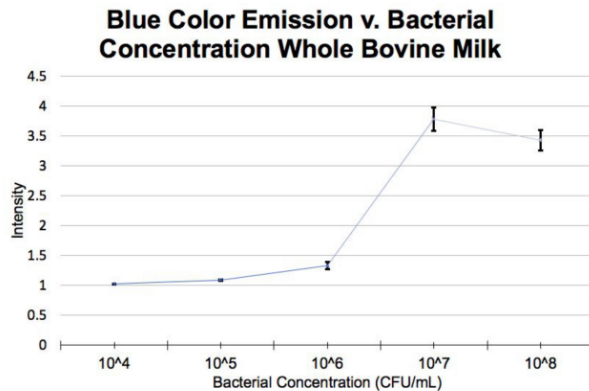


Figure 19. Graph depicting the calculated RGB ratio for different concentrations of *E. coli* induced with whole bovine milk.

(b)

Figure 3: Graphs depicting the calculated RGB ratio for various concentrations of *E. coli* induced with (a) DHBM and (b) whole bovine milk.

3.6 Lower Limit of Detection Challenges

Although previous work [3] has demonstrated the viability of the X-gal alginate hydrogel detection method, the accepted lower limit of detection (LOD) requirement for bacterial pathogens of 10^4 CFU/mL [6] has not been reliably achieved for *E. coli* in this system. The senior design team that first used an alginate hydrogel system with X-gal and β -galactosidase reported their lower LOD as 10^6 CFU/mL [33]. Optimizing various system parameters using Taguchi designs allowed for a 10^2 CFU/mL lower LOD, however this LOD was binary. The system could not differentiate between 10^2 and 10^3 CFU/mL, making it ineffective for rejecting breast milk samples with 10^4 CFU/mL while accepting 10^3 CFU/mL [3]. Using an updated image analysis mechanism, last year's senior design team achieved a 10^4 CFU/mL lower LOD, but this was only for pathogens in water [35]. It is imperative that MilkGuard consistently achieves a 10^4 CFU/mL (and ideally lower) LOD to be acceptable for usage at milk banks.

3.7 Rationale for Current Work

To address current challenges of the MilkGuard system, our project focuses on the development of a computer-aided design (CAD) model, a simulation-aided geometry optimization, a colorimetric analysis algorithm, and a mobile phone application. Our work aims to improve the sensitivity and usability of the X-gal alginate hydrogel system to more precisely and accurately detect *E. coli* in donated breast milk at milk banks. A realistic, dynamic CAD model allows for cost-savings and waste-reduction compared to an equivalent amount of physical laboratory experiments. The CAD model additionally allows for the easy collection and storage of experimental data, and can be used, as demonstrated below, to optimize subsystems. Automating colorimetric analysis with a computer algorithm programmed into a mobile application is a reliable, cost-effective way to achieve highly sensitive results. Due to the prevalence of smartphones, use of mobile phone applications in low-resource conditions is common [36-39], and suggests that the MilkGuard system may be adapted in the future for use in such settings.

Chapter 4: Materials & Methods

4.1 MilkGuard Subsystems

To reach the target sensitivity of 10^4 CFU/mL, MilkGuard was split into two subsystems. First, the optimization of the biosensor parameters would improve the color-producing efficacy of our system, which would bring us closer to our goal. Computer simulations were determined to be the most effective way to optimize the MilkGuard biosensor.

Another way to reach our target sensitivity was to improve the color-analysis component of the MilkGuard system. A mobile application was developed to improve the ease of analysis. The mobile application utilized a color-analysis algorithm that was improved upon to increase sensitivity. Several approaches were considered, but the final improvements are listed in following sections.

4.2 Simulation Materials

4.2.1 Chemical & Biological Reagents

E. coli strain SCU-104, Luria Bertani broth, N,N-Dimethylformamide, medium-viscosity alginic acid, and β -galactosidase were purchased from Sigma-Aldrich (St. Louis, MI, USA). The B-PER Direct Bacterial Protein Extraction Kit and X-gal were procured from Thermo Fisher Scientific (Waltham, MA, USA). All other reagent grade chemicals were provided by the Bioengineering Department at Santa Clara University, (Santa Clara, California, USA). Further details and lot numbers are described in previous literature [3].

4.2.2 COMSOL Multiphysics

COMSOL Multiphysics v.5.5 was used to develop a 2D virtual model of our biosensor based on parameters established in previous experiments. A space-dependent Transport of Diluted Species module to model diffusion and a Chemistry module to model the reaction of beta-galactosidase and X-gal were incorporated into the COMSOL simulation.

4.2 Simulation Methods

4.2.1 Laboratory Methods

As described in detail in previous literature [3], *E. coli* were cultured, grown to appropriate optical density (OD), and induced for lac operon expression using breast milk samples. After incubating the breast milk-induced *E. coli* samples overnight, the bacteria were harvested, resuspended, and used to create ladders of known bacterial concentrations in breast milk. Samples were then lysed with B-PER protein extraction solution to extract β -galactosidase from the *E. coli*.

The alginate hydrogel microcapsules were fabricated as described in section 3.2.

4.2.2 Simulation Geometry

The geometry in our simulation is a 2D representation of the alginate hydrogel biosensor previously developed. A 2D simulation was chosen for reduced computational complexity and for compatibility with available data. The spherical capsule alginate hydrogel biosensor is represented by two concentric circles (“capsule”). The space between the concentric circles is an explicitly defined reaction space (“membrane”). Previous research [3] suggests that X-gal is sparingly or insoluble in breast milk. Thus, the hydrolysis reaction of X-gal is isolated primarily to the surface of the hydrogel capsule represented by the space between the concentric circles.

4.2.3 Simulation Parameters

A transport of diluted species model of existing biosensor data was created in COMSOL Multiphysics v.5.5. The transport is governed by Fick’s Second Law of Diffusion, given in Eq. 1. Michaelis menten kinetics for enzymatic reactions given in Eq. 2 are used to model the hydrolysis of X-gal. The reaction rate R_i from Eq. 2 is then substituted into the reaction rate term R_i in Eq. 1 to yield Eq 3. Various model parameters are defined in Eq. 4. The gradient term in Eq. 1 is expanded and parameters from Eq. 4 are then substituted into Eq 1 to yield Eq. 5

The terms in Eq. 5 can be rearranged to contain the Thiele Modulus for spherical capsules given in Eq. 6. Substituting the Thiele Modulus for spherical capsules into Eq. 5 then yields Eq. 7.

$$\begin{aligned}
(1) \quad & \frac{\partial S}{\partial t} = D \nabla^2 S + R_i \\
(2) \quad & r_s = \eta \frac{V_m'' [S_s]}{[S_s] + K_m} \\
(3) \quad & \frac{\partial S}{\partial t} - D_e \left(\frac{\partial^2 [S]}{\partial r^2} + \frac{2}{r} \frac{\partial [S]}{\partial r} \right) = \frac{V_m'' [S]}{[S] + K_m} \\
(4) \quad & \bar{S} = \frac{[S]}{[S_s]}; \bar{r} = \frac{r}{R}; \beta = \frac{K_m}{[S_s]} \\
(5) \quad & \frac{1}{S_e} \frac{\partial \bar{S}}{\partial t} - \left(\frac{\partial^2 \bar{S}}{\partial \bar{r}^2} + \frac{2}{\bar{r}} \frac{\partial \bar{S}}{\partial \bar{r}} \right) = \left(\frac{V_m'' R^2}{S_e D_e} \right) \frac{\bar{S}}{\bar{S} + \beta} \\
(6) \quad & \Phi = R \sqrt{\frac{V_m'' / K_m}{D_e}} \quad \text{Thiele Modulus} \\
(7) \quad & \frac{1}{S_e} \frac{\partial \bar{S}}{\partial t} - \left(\frac{\partial^2 \bar{S}}{\partial \bar{r}^2} + \frac{2}{\bar{r}} \frac{\partial \bar{S}}{\partial \bar{r}} \right) = \Phi^2 \frac{\bar{S}}{(\bar{S} + \beta) \left(\frac{1}{\beta} \right)}
\end{aligned}$$

The Thiele modulus for spherical capsules relates the kinetic (V_m'' / K_m), diffusive (D_e) and geometric (R) parameters. While Eq. 7 can be used to effectively model diffusion, the individual components of the Thiele modulus cannot be effectively experimentally determined, and therefore cannot be used to effectively model the reaction velocity. Instead, an alternative mechanism is used to relate kinetic, diffusive, and geometric parameters. Data for Michaelis-Menten kinetics of the hydrolysis of X-gal with β -galactosidase were collected for free, un-encapsulated X-gal. These experimentally derived values V_m and K_m are used to approximate the model's kinetic parameters. To account for the diffusion-limiting effect of X-gal encapsulation, values relating hydrogel capsule radius r and the reduction in reaction velocity η ("effectiveness factor") were collected experimentally. MATLAB Curve Fitting was used to generate a relationship between capsule radius and effectiveness factor η . The resulting curve is power function

$$(8) \quad \eta = Ar^B + C$$

where $A = 0.2429$, $B = 0.1243$, and $C = 1.033$. Figure 4 gives a model of the effectiveness function. Thus, the complete reaction rate in the model is given by

$$(9) \quad \text{rate} = \frac{V_{max}[xgal]}{K_m + [xgal]} \times (Ar^B + C)$$

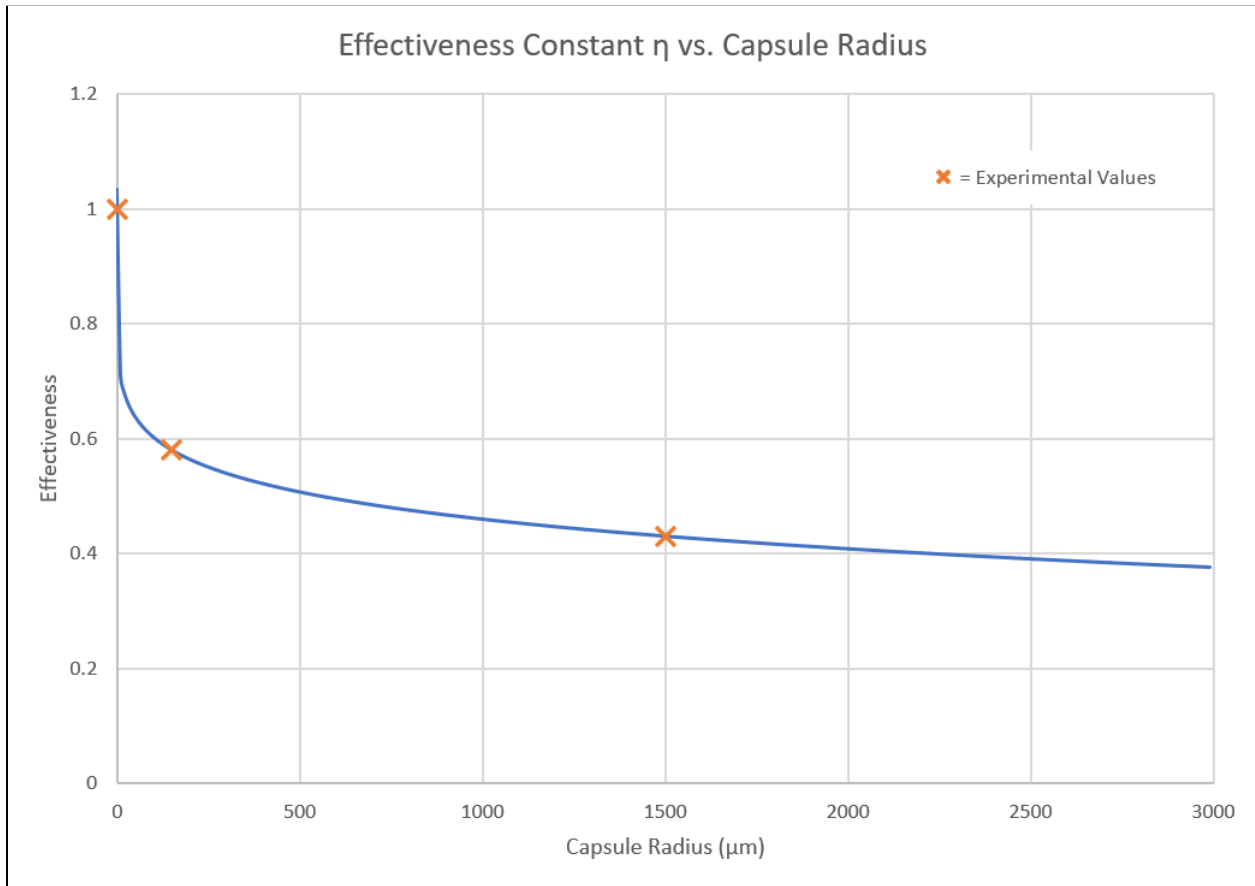


Figure 4: Effectiveness constant as a function of capsule radius, from experimentally derived values.

The diffusion constants and initial concentrations in the model are given in Table 1.

Table 1: Simulation inputs for COMSOL biosensor model.

	X-gal	blue precipitate
D_{membrane} (m ² /s)	$1 \times 10^{-12} (D_A)$	$5 \times 10^{-10} (D_B)$
D_{capsule} (m ² /s)	$1 \times 10^{-12} (D_A)$	$5 \times 10^{-10} (D_B)$
D_{bulk} (m ² /s)	0	1×10^{-6}
Initial concentration _{membrane} (mol/m ³)	1	0
Initial concentration _{capsule} (mol/m ³)	1	0
Initial concentration _{bulk} (mol/m ³)	0	0

Mass balances around the control volume with membrane thickness δ are shown in Eq. 10 and Eq. 11.

$$(10) \quad N_A \left(\frac{\text{mol}}{\text{s}} \right) = -4\pi r^2 D_{BA} \left[\frac{d[C_A]}{dr} \right]_{r=\delta} - \text{rate} + 4\pi r^2 D_{mA} \left[\frac{d[C_A]}{dr} \right]_{r=0}$$

$$(11) \quad N_B \left(\frac{\text{mol}}{\text{s}} \right) = -4\pi r^2 D_{BB} \left[\frac{d[C_B]}{dr} \right]_{r=\delta} + \text{rate} - 4\pi r^2 D_{mB} \left[\frac{d[C_B]}{dr} \right]_{r=0}$$

There were no Dirichlet nor Neumann boundary conditions explicitly defined in the COMSOL simulation to solve the transient concentration profiles. Rather, the boundary conditions were driven by fluxes.

Since X-gal solubility is low in the aqueous bulk solution (breast milk), the bulk diffusion coefficient was set to zero. This forced a zero flux condition at the outer membrane interface. Although the reaction rate is a lumped rate of two-phase (solid substrate/liquid enzyme) and one-phase (solubilized substrate/liquid enzyme) reaction mechanisms, the rate was simplified in the model to assume the reaction rate occurs in one phase. The two-phase system and insolubility of X-gal in the bulk solution are reflected in the differences in substrate diffusivity between the membrane and capsule domain; X-gal substrate diffusivity is set two orders of magnitude lower than that of the water-soluble blue reaction precipitate.

4.2.4 Geometry Optimization

A geometry-optimization experiment was conducted with the completed COMSOL model to develop a theoretical basis for future laboratory experiments. This model allows this research team to streamline laboratory experimental trials to reduce the cost and production of hazardous waste.

The optimization explored three variables: 1) the radius of each alginate hydrogel capsule (“biosensor radius”), 2) the number of capsules per sample (“capsule count”), and 3) the total alginate hydrogel volume (“biosensor volume”). Capsule radii were varied from 200 to 1,500 μm , approximately the range of microcapsules that can be reliably produced with extrusion-based microfluidics. Capsule counts examined were 1, 5, 10, and 25 capsules. Raising the capsule count above 25 results in long computation times and lowers the cost-effectiveness of the manufacturing process. The optimization examined total alginate hydrogel volumes of 1 μL , 10 μL , 20 μL , 30 μL , etc. up to a maximum of 100 μL . A spherical alginate hydrogel biosensor geometry was retained throughout the optimization for ease of production.

To reduce the total number of computations while maintaining investigative results, a total biosensor volume was selected first. Then, the radii required to additively achieve that total volume with 1, 5, 10 and 25 capsules were calculated. These radii values were rounded to the nearest multiple of 5, based on the limitations of the level of precision of extrusion-based coaxial jetting processes. All values tested in COMSOL are provided in Table 2.

Table 2: Radius values (μm , shown in white) tested in COMSOL, calculated to fit into specific volume categories (light blue) for each capsule count (dark blue).

Capsule Radii (μm) Tested in COMSOL				
Volume Category (μL)	Capsule Count			
	1	5	10	25
1	625	375	300	210
10	1350	775	625	450
20	1700	975	775	575
30	1925	1125	900	650
40	2125	1250	975	725
50	2300	1325	1050	775
60	2425	1425	1125	825
70	2550	1500	1175	875
80	2675	1575	1250	925
90	2775	1625	1300	950
100	2875	1675	1325	975

4.4 Mobile App Materials

A mobile application, Milkguard, was developed for Android smartphones. The Android Operating System was chosen over Apple's iOS since Android devices are usually more cost-effective [40], and are more widely available to our target consumers.

Since the app was implemented in the cross-platform React Native language, small modifications to the source code would allow iPhone users to use the MilkGuard app as well [41]. Besides being readily adaptable for both iOS and Android operating systems, the React Native language is also the best choice for starting app development from scratch [42]. Its combined simplicity, computational efficiency, and compatibility with JavaScript [43] make React Native the ideal choice as our mobile application development language.

Most of the application features (buttons, navigation menu, and design & user interface elements) were implemented from the Expo Software Development Kit [44], but the color analysis software component was downloaded as a Native Module from npm.js [45]. The chosen `react-native-image-colors` module was the most user-friendly and highest rated color analysis module on the NPM open source repository [45].

The `react-native-image-colors` module returns RGB values for the selected portion of the image by accessing the palette class on Android [46], and can return the “dominant,”

“average,” “muted,” “vibrant,” color scheme for a selected image, but the Milkguard app only uses the “average” result. The `getColor()` function averages every n pixels in the selected image.

4.5 Mobile App Methods (long section)

4.5.1 RGB Color Balance

Since every brand of smartphone captures color slightly differently [47], our mobile application performs color balance before continuing with colorimetric analysis. Humans have a psychological ability to maintain color constancy in different lighting environments [48], but computers require additional processing to do the same [49]. Several color balance algorithms exist, such as those for improving diagnosis via color-stained tissue in anatomic pathology [50] for computer vision applications. The MilkGuard app uses a simple linearization color balance algorithm designed for general use [51]:

$$\begin{bmatrix} R \\ G \\ B \end{bmatrix} = \begin{bmatrix} 255/R'_w & 0 & 0 \\ 0 & 255/G'_w & 0 \\ 0 & 0 & 255/B'_w \end{bmatrix} \begin{bmatrix} R' \\ G' \\ B' \end{bmatrix}$$

The returned RGB values display $R = 255$, $G = 255$, and $B = 255$ for the designated standard white.

4.5.2 Conversion to HSL Color Space

We then convert the color balance from RGB to HSL (defined below) for improved colorimetric analysis. Because the RGB color space was designed for the now-prevalent tri-color LCD displays [52], it is the most common way to represent color digitally, but it is not ideal for biological image analysis [53]. The RGB values are converted to HSL according to the following algorithm [54]:

$$R' = R/255$$

$$G' = G/255$$

$$B' = B/255$$

$$C_{max} = \max(R', G', B')$$

$$C_{min} = \min(R', G', B')$$

$$\Delta = C_{max} - C_{min}$$

$$H = \begin{cases} 0^\circ & , \Delta = 0 \\ 60^\circ \times \left(\frac{G'-B'}{\Delta} \bmod 6\right) & , C_{max} = R' \\ 60^\circ \times \left(\frac{B'-R'}{\Delta} + 2\right) & , C_{max} = G' \\ 60^\circ \times \left(\frac{R'-G'}{\Delta} + 4\right) & , C_{max} = B' \end{cases}$$

$$S = \begin{cases} 0 & , \Delta = 0 \\ \frac{\Delta}{1-|2L-1|} & , \Delta \neq 0 \end{cases}$$

$$L = \frac{C_{max} + C_{min}}{2}$$

In the HSL color space, HSL is an abbreviation for Hue, Saturation, Lightness (or Luminance, or Luminosity). HSL is interchangeably known as HSB, which stands for Hue, Saturation, Brightness, but the values are identical.

- Hue: identifies the base color, independent of shade or tone. In optics, hue is directly correlated to the wavelength of light. Under white lighting circumstances, adjusting the brightness does not affect the hue [55].
- Saturation: identifies the pureness and intensity of a color. As saturation decreases, that color looks more and more like gray. A black and white image has a saturation value of 0 (zero) [55].
- Lightness: identifies the brightness of a color. A lower value corresponds to a color that is closer to black, and a higher value is closer to white [55].

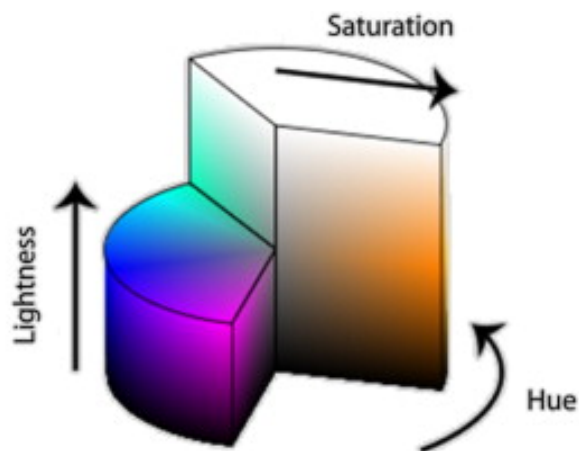


Figure 5: An HSL color cylinder model showing the corresponding dimensions for Hue, Saturation, and Lightness [56].

The HSL color space is superior to RGB for color analysis, because RGB is often “unable to produce sufficient information for Digital Image analysis” [57]. HSL provides the most consistent numerical regression information [58], which our app needs. Other colorimetric analysis diagnostic tools also prefer the HSL color space, such as an algorithm for melanoma detection [59].

Finally, the HSL color space is more scientifically intuitive for our assay. In the presence of *E. coli*, and therefore the β -Galactosidase enzyme, X-Gal is cleaved into colorless galactose plus 5-bromo-4-chloro-3-hydroxyindole, which oxidized into 5,5'-dibromo-4,4'-dichloro-indigo. The indigo product has maximum absorbance at 650 nm, and thus it appears blue [60]. Against our white wellplate, differing concentrations of the indigo-colored substrate directly affect the Saturation and Lightness of the sample color, but not the Hue, since the reflectance and absorbance wavelength values of the 5,5'-dibromo-4,4'-dichloro-indigo do not change. Therefore, our color regression only depends on the S and L of the HSL colorspace (the lightness/darkness and intensity of the given 5,5'-dibromo-4,4'-dichloro-indigo blue). The RGB color space unnecessarily complicates this relationship through varying proportions of the red, green, and blue components of the sample color, which are not easy to decipher.

4.5.3 HSL Distance

The obtained HSL values are then used to calculate the Euclidean distance between the sample color and pure white. Since the identity of the target chemical product does not change, Hue is assumed to hold constant. Thus the Euclidean distance is calculated from the Lightness and Saturation components only.

Calculating the Euclidean distance in color spaces (including RGB [61]) is a common technique to obtain single numerical results to be used in analytical regression [62]. This technique is effective for small color differences, such as for determining the level of tomato ripeness [63], but ineffective for large color differences [64]. Fortunately, our app only needs to differentiate between various shades of blue which are relatively close in the HSL color space.

$$\text{Color Distance} = \log \sqrt{S^2 + L^2}$$

The logarithm of calculated distance value is obtained to consolidate range. Then, the transformed color distance values are plotted against *E. coli* concentrations. The same procedures applied to other sets of laboratory data.

Chapter 5: Results

5.1 Simulation Outcomes

5.1.1 Comparison to Experimental Results

The generated COMSOL model reflects behavior observed in experimental data. In laboratory experiments, visualization of X-gal with phase-contrast microscopy showed that X-gal crystal concentration appears to decrease only near the surface of the microcapsules after 2 hours of reaction time. Additionally, the intensity of the blue precipitate continues to increase up to around 24 hours of incubation [65]. This suggests that the diffusion of X-gal through the hydrogel capsule is relatively slow, and that X-gal concentration at the center of the capsules should not change much throughout the six hour simulation. Parameters were selected to maintain initial X-gal concentration of 1 g/m^3 at the center of capsules of $1500 \text{ }\mu\text{m}$ radii. For capsules of smaller radii (approximately $<700 \text{ }\mu\text{m}$) the concentration at the center of the bead begins to decrease by six hours of reaction time.

Figure 6 shows bisected hydrogel capsules removed from breast milk samples spiked with *E. coli* after specific incubation times are shown with corresponding frames from the COMSOL model. Capsules removed and bisected after about 5 minutes of incubation show no visible blue precipitate. After 30 minutes of incubation, a light hue is observed at the surface of the capsule with a very faint hue present at the center of the capsule. After 60 minutes of incubation, precipitate concentration has become more uniform throughout the capsule.

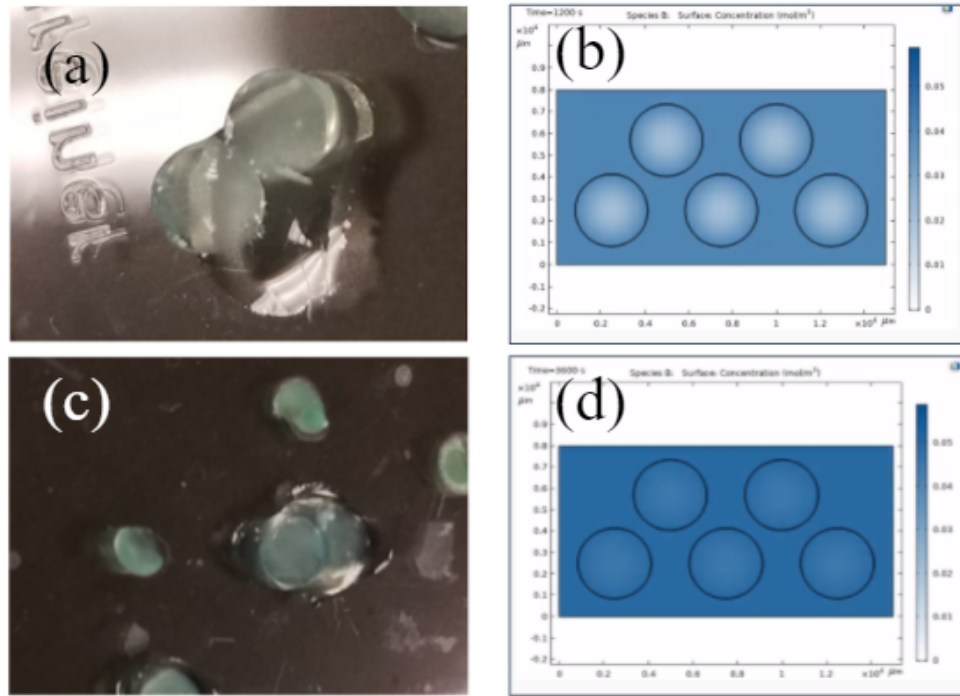


Figure 6: Comparison of experimental data and COMSOL model surface concentration outputs for blue reaction precipitate. a) Experimental after 30 mins incubation, b) COMSOL output at 30 minutes reaction time, c) Experimental after 60 mins incubation, d) COMSOL output at 60 minutes reaction time. Figure 6a and 6c from Madamba, 2019 [65].

5.1.2 Geometry Optimization

The simulation results suggest that the reaction progression is most efficient (i.e. when blue color change for a given volume of X-gal/alginate hydrogel capsule is most rapid) in capsules with smaller radii. In other words, if total capsule volume is fixed, the system's time-to-result decreases when that total volume is divided up into a greater number of capsules (see Figure 7). This trend was observed across all time indices and for all fixed capsule volumes.

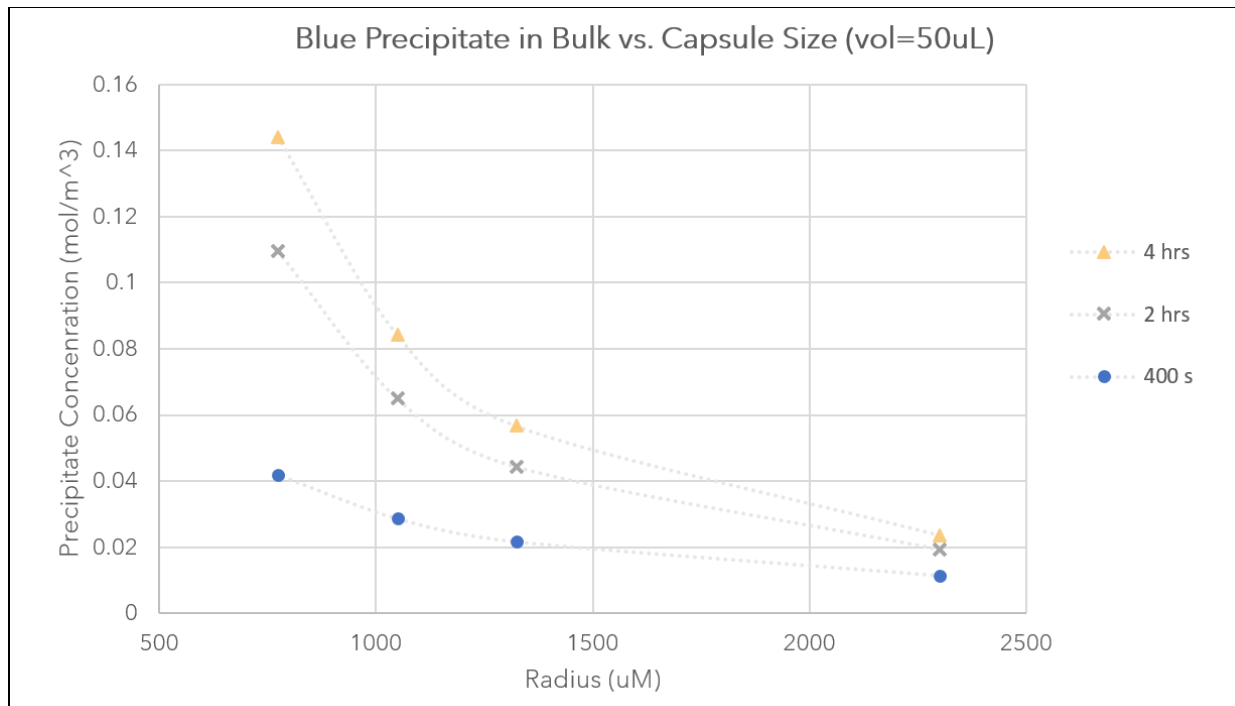


Figure 7: Reaction precipitates concentration in milk samples (i.e. outside of the biosensor capsule) as a function of capsule radius at selected time indices. The total capsule volume is held constant at 50 μL for all data points in this figure. Capsule radii are varied with fixed capsule volume by modulating the number of capsules used per sample. From left to right, capsules counts for corresponding radii values are 25, 10, 5, and 1 capsules per sample. The results suggest that spherical capsules with smaller radii have the most efficient reaction progression.

When capsule count is held equal and volume is varied by modulating capsule radius, greater total capsules volumes produce the most rapid color change (see Figure 8). This finding was consistent across all capsule counts.

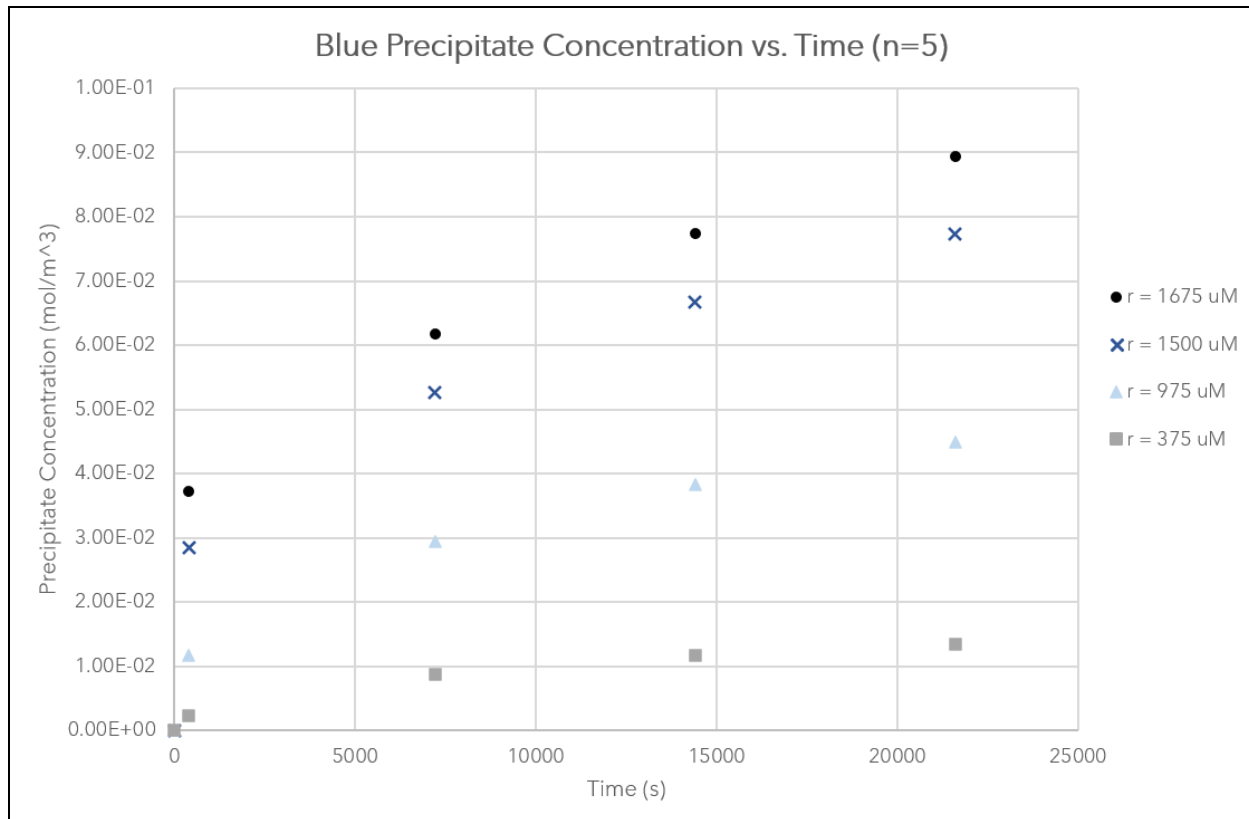


Figure 8: Reaction precipitate concentration over time for capsules of selected radii. Results indicate that greater total capsule volumes produce more rapid results.

Taken together, the geometry simulation suggests that ideal biosensor geometry for this system would be a high number of alginate hydrogel capsules (and therefore high total biosensor volume) with the smallest radii that can be reasonably manufactured. The total capsule volume will be limited by the cost of X-gal. The size of the capsule radii will be limited by manufacturing costs.

5.1.3 Future Work

More research is needed to determine more precise diffusivity constants for the transportation of X-gal and the blue reaction precipitate product. Once determined, these values can easily be added to the COMSOL model. In-lab experiments, informed by the results of the COMSOL model, should be performed to confirm biosensor geometry optimization. The results of in-lab experiments should then be considered against

material and manufacturing cost considerations to produce a product that is sensitive, rapid, and affordable for breast milk banks.

The existing COMSOL model can be iterated to incorporate additional factors that potentially impact bacteriological results. For example, it was determined that alginate hydrogel bulk degradation was negligible over the time period studied in this application [66], but degradation may become an important variable to include if the hydrogel material is altered to reach the required lower limit of detection [6].

5.2 Color Analysis / Mobile App Results

Images of colorimetric ladders obtained from previous teams are shown in Figure 2. The corresponding HSL values are marked on the HSL color cylinder model. As predicted by theory, Hue stays relatively constant, while Saturation and Lightness vary, producing points that lie on a line, which can be analyzed via obtaining the color distance value.

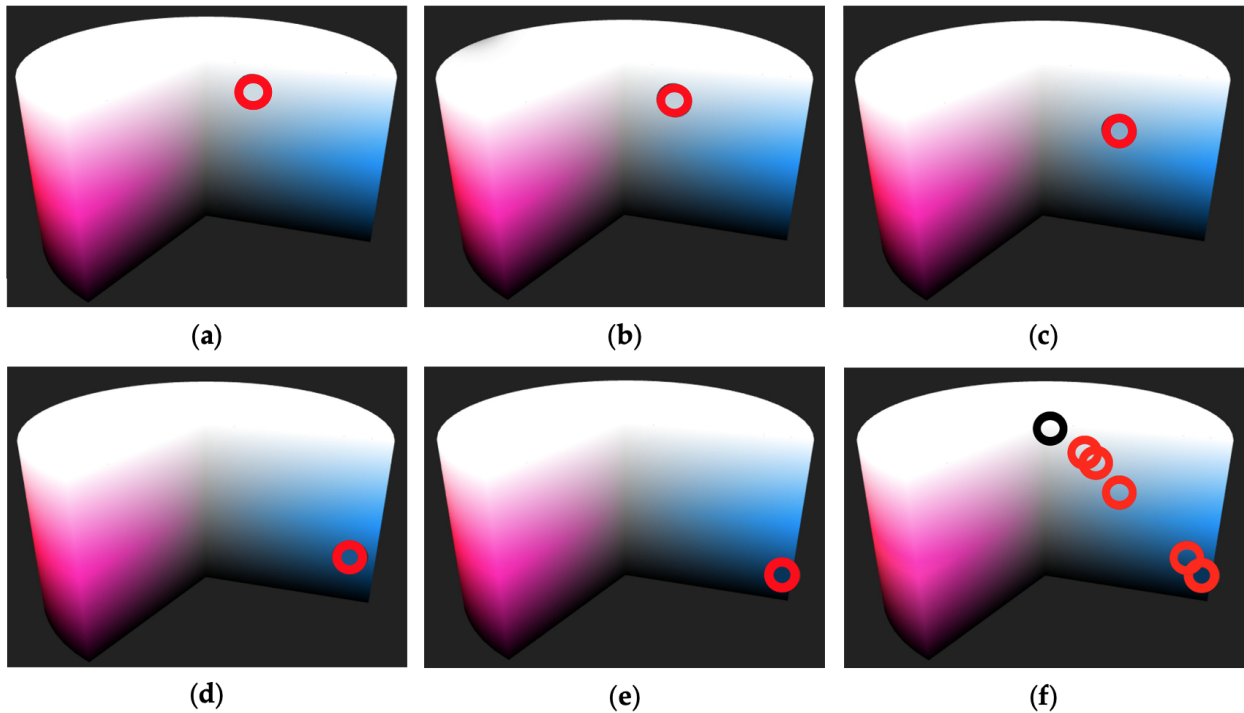


Figure 9: Induced blue color represented on the HSL color space cylinder model for (a) 10⁴ CFU/mL, (b) 10⁵ CFU/mL, (c) 10⁶ CFU/mL, (d) 10⁷ CFU/mL, (e) 10⁸ CFU/mL. (f) All concentrations shown, with the black circle representing pure white.

The combination of colorimetric analysis strategies yielded the following graphical results, as seen in Figure 10.

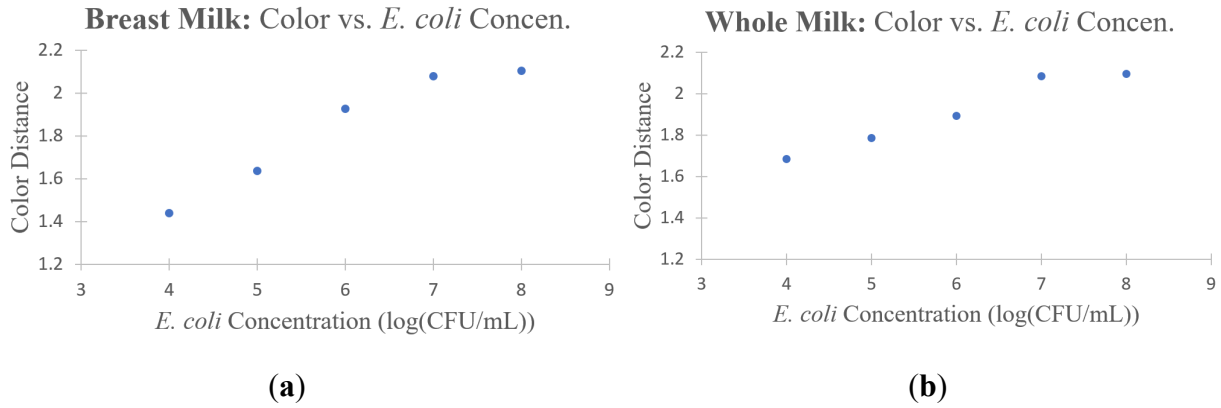


Figure 10: Graphs depicting the calculated Color Distance Values for various concentrations of *E. coli* induced with (a) DHBM and (b) whole bovine milk. Image data obtained from previous MilkGuard Team’s laboratory results.

The two graphs demonstrate differentiable colorimetric sensitivity from 10^4 – 10^7 CFU/mL range. See further analysis on the graphs in Section 6.2.

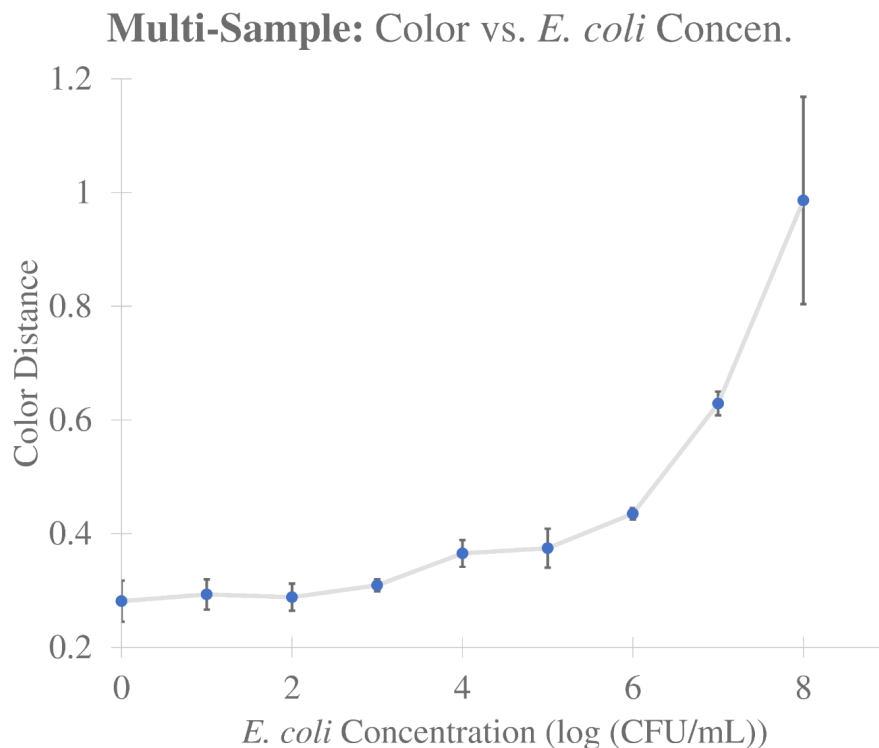


Figure 11: Graph depicting the calculated Color Distance Value for various concentrations of *E. coli* induced with DHBM in clear wellplates. Image data obtained from previous MilkGuard Team’s laboratory results (n = 3).

The graph above demonstrates differentiable colorimetric sensitivity between 10^4 and 10^5 CFU/mL, and beyond 10^6 CFU/mL. See further analysis on the graphs in Section 6.2.

Figure 12 shows a series of screenshots that depicts the workflow of the MilkGuard app, which makes it intuitive for the user to access the color-analysis algorithm described above. From the home screen (a) the user can choose to view history or run a test. After the instructions screen (b), the user chooses an image to analyze from images stored in local memory (not shown) or from the in-app camera (c). The user then chooses a specific area of the selected picture (d) to analyze by moving the corners of the box to focus on the area of interest. The confirmation page (f) allows the user to check the image quality before proceeding. Steps (b–f) are repeated for choosing the “Standard White” for color balance (selection of standard white not shown). The results screen (g) displays the bacterial concentration. The user can edit the date of the sample and include extra notes for reference, before storing into history (h). Steps (a–g) are repeated for a new milk sample.

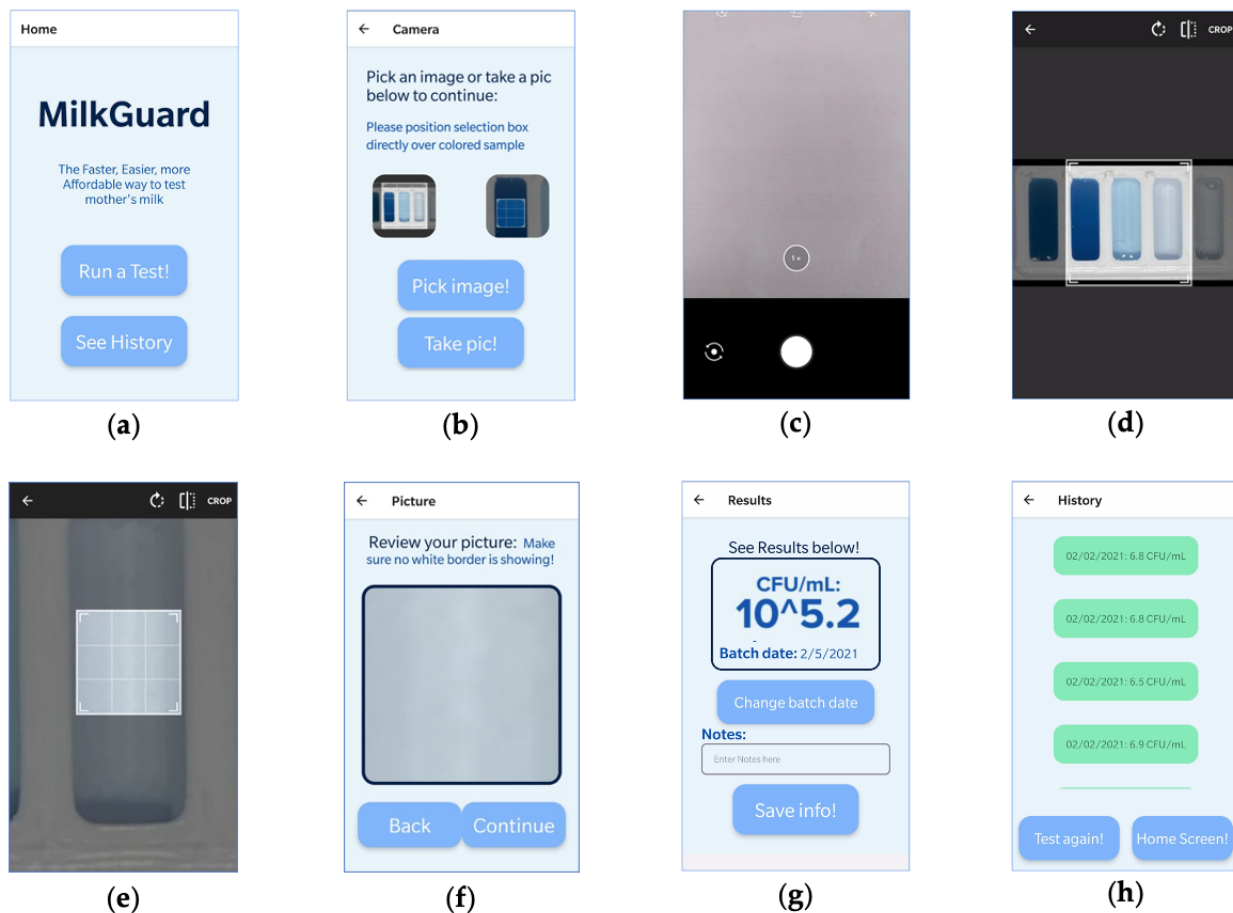


Figure 12: Diagram showing screenshots from the MilkGuard app. (a) Home screen with options to run a test or see history of tests. (b) Instructions screens with options to obtain image via camera or image library. (c) Screenshot of camera. (d) Selection box for focusing on area of interest. (e) Selection box correctly placed over color. (f) Confirmation screen shows selected image to be analyzed. (g) Results screen with options to change or enter information. (h) History screen with information on previous test results.

Chapter 6: Discussion and Recommendations

6.1 Biosensor Simulation & Optimization

COMSOL simulation of biosensor parameters provided a low-cost method to optimize MilkGuard's color-producing speed and efficacy. Through the rounds of simulations, we discovered that biosensor capsules with greater volume produce more rapid results, which faster detection of *E. coli* contamination. More rapid results can also be observed by increasing the surface area of the biosensor, with all other factors held constant, which can be achieved by dividing the biosensor hydrogel into as many portions of micro-encapsulated spheres as manufacturing technologies allow. Future teams would have to find an optimization between biosensor volume and individual size to achieve the goals of MilkGuard, while staying within the constraints of chemical reagent and manufacturing costs.

Perhaps the most significant contribution of COMSOL simulation is the proof of concept that computer-aided modeling could be used to optimize for the MilkGuard sensor. Running simulations on a computer is much more economical and environmentally friendly than producing hundreds or thousands of physical sensors with varying parameters, and testing each one. Costs have been especially reduced in avoiding the use of X-gal in physical sensors, due to the high cost of the reagent. By running simulations, instead of producing, testing, then disposing of multiple batches of biosensors, production of hazardous waste has been avoided. We have built a simulation framework that future teams can utilize to further improve on the color-producing efficacy of the MilkGuard sensor. The simulation gives MilkGuard the information and tools to effectively and efficiently create a product that achieves our required lower limit of detection to improve the health and safety of infants.

6.2 Mobile App & Color Analysis Algorithm

The addition of several algorithmic improvements to the previous team's color-analysis algorithm resulted in more sensitive and consistent results. Figure 13 compares the graphical results of last year's and this year's color analysis algorithm. The two algorithms were applied to the exact set of images, but they yielded different results. When comparing the results of analyzing the 3D printed white well plate (Figure 2), we can see a difference between the graphs

of this year and last year, for both the DHBM and whole bovine milk images. In the graph from last year, we see an insignificant difference between the 10^4 and 10^5 CFU/mL values. However, our new algorithm yielded a noticeable difference between those two values, and presented linearity between 10^4 and 10^7 CFU/mL values, which is very useful for building linear regression curves.

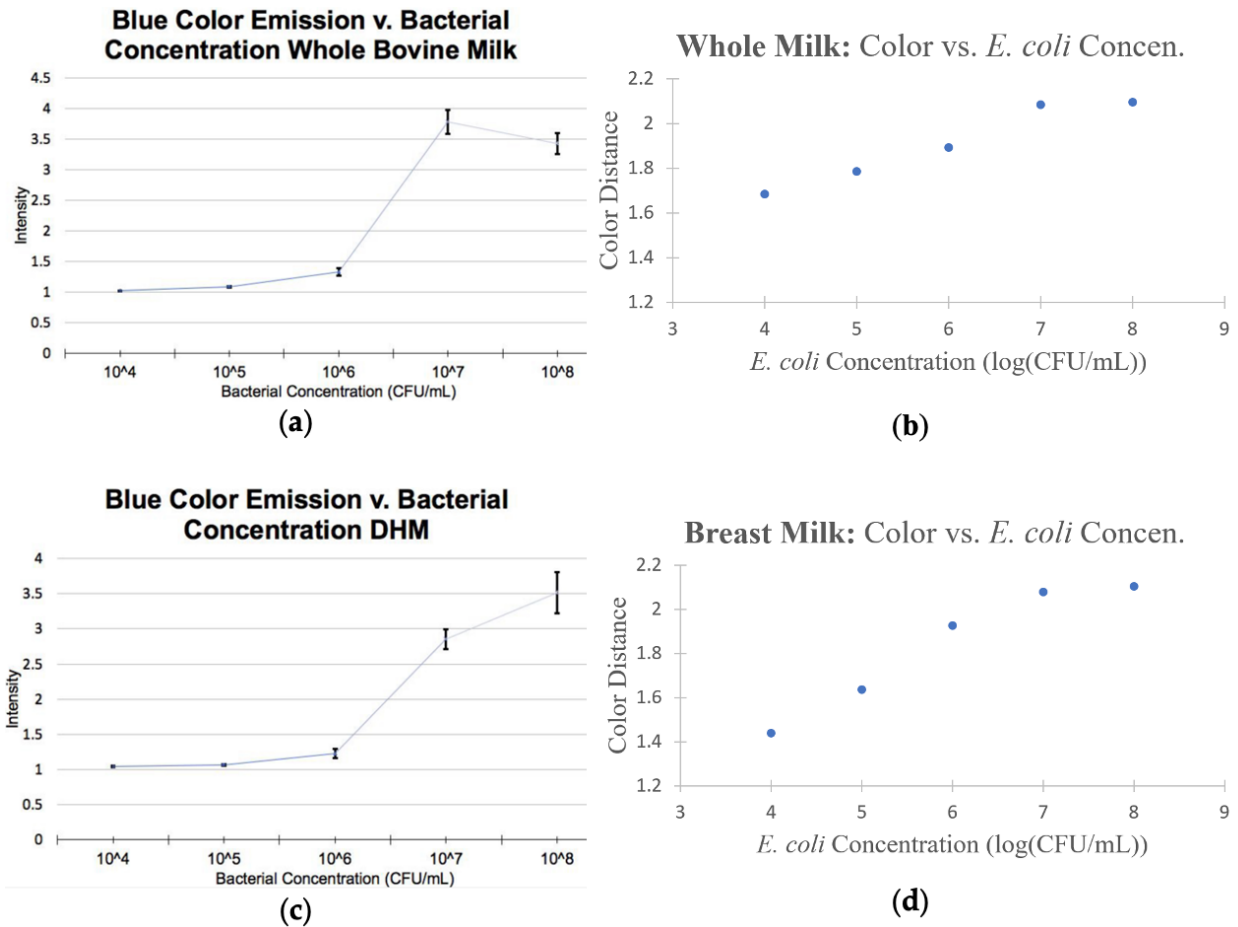


Figure 13: Graphs depicting the calculated color values for various concentrations of *E. coli* induced with (a) whole bovine milk, analyzed using previous algorithm, (b) whole bovine milk, analyzed using new algorithm, (c) DHBM, analyzed using previous algorithm, (d) DHBM, analyzed using new algorithm. Analysis performed on the same set of image data obtained from previous MilkGuard Team’s laboratory results.

In analyzing the series of clear well plates (not shown), our new algorithm also increased the sensitivity in our region of interest (10^4 CFU/mL). Whereas the previous algorithm yielded an insignificant difference between 10^3 and 10^4 CFU/mL values, our new algorithm shows a

significant difference, as indicated by the error bars. The increased sensitivity of our new algorithm around the target region (the HMBANA’s recommended lower limit of detection standard of 10^4 CFU/mL) shows the improved efficacy of our system. The improved detection of low but still potentially harmful concentrations of *E. coli* in DHBM at milk banks may promote the health of infants who need a safe milk source.

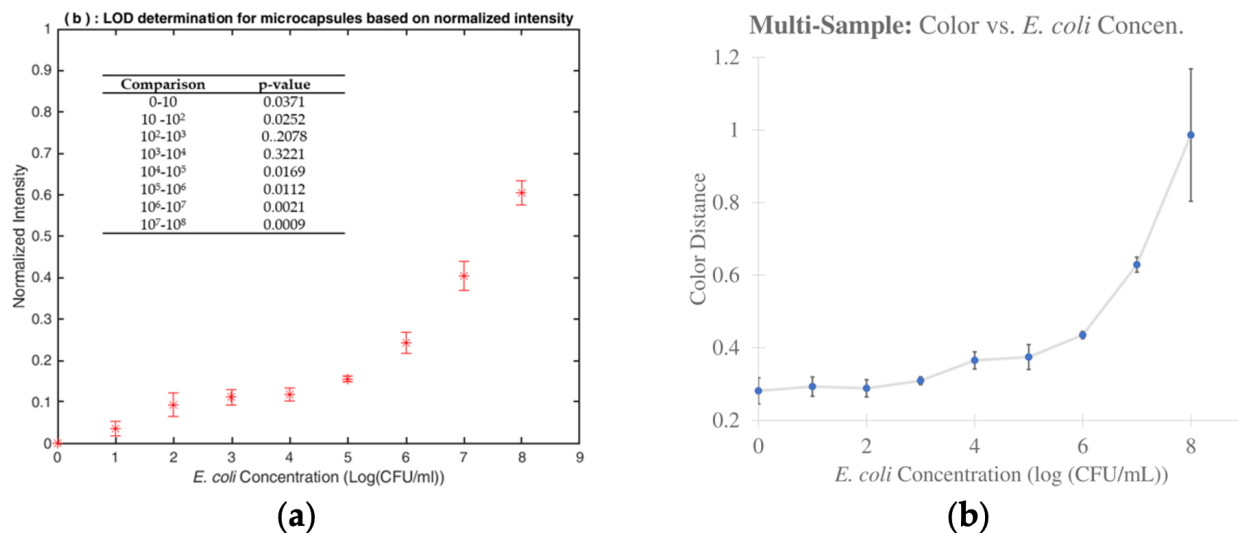


Figure 14: Graphs depicting the calculated color values for various concentrations of *E. coli* induced with DHBM in clear wellplates (a) before and (b) after applying color balance, HSL conversion, and color-distance regression. Analysis performed on the same set of image data obtained from previous MilkGuard Team’s laboratory results (n = 3).

The development of the mobile app greatly simplifies the process of colorimetric analysis for the end user. Before, the user would need to take a picture of the resulting milk sample, upload the image onto a computer, use the ImageJ software to obtain the RGB values, and calculate the color intensity ratio before comparing it with the standardized regression curve. This was a complicated process. With the app, the milk bank technician can now perform all these tasks right on a smartphone within minutes, guided by the instructions and workflow provided by the app. The app contains a user interface that is minimalistic and attractive to use, and the buttons are big and easy to tap. The mobile app is a product that could be highly distributable via Apple App Store or the Google Play Store. Altogether, the MilkGuard app greatly increases the usability of the milk system and removes obstacles the user may face when

trying to utilize our novel color analysis algorithm. We are hopeful that this improvement increases the accessibility of our product to milk banks in need.

6.3 Cost Considerations

The system discussed in this paper may offer milk banks a cost-effective alternative to the current practice of bacteriological testing at external laboratories [67]. Estimates of assay cost vary based on biosensor geometry, X-gal concentration, and B-PER bacterial extraction concentration but all yield cost-per-sample estimates of less than \$1. This suggests that the MilkGuard technology could significantly reduce the costs of bacteriological testing at milk banks, which currently range from \$35-81 per 100-200 oz of breastmilk [8]. Multiple studies [68-70] have documented the cost-effectiveness of point-of-care testing, particularly when testing mechanisms are low-cost and reliable.

6.4 Next Steps

6.4.1 Remaining Challenges

Despite our accomplishments this year, there are still important improvements to be made on the MilkGuard System. Through processes described above, both the biosensor geometry and improved image analysis algorithm developed this year bring MilkGuard closer to achieving the HMBANA's 10^4 CFU/mL lower limit of detection requirement. However, due to the lack of lab access this year, we have not been able to physically test and confirm whether the suggested geometry optimization and algorithmic improvements will consistently allow us to reach this level of sensitivity. Similarly, a related challenge remains—that of achieving consistent lighting while capturing images of milk samples. Previous teams have developed a light box as described in Section 3.5. However, we have yet to test whether that will still be necessary, given our implementation of the color-balancing algorithm. Future teams must perform tests on a large number of samples to confirm that it will adequately provide consistent image analysis in a low-resources setting. Otherwise, the light box will continue to be required as part of the MilkGuard system.

A few challenges were not addressed in this paper. The MilkGuard team had observed a batch-to-batch variation in β -galactosidase expression in *E. coli*. In other

words, different strains of *E. coli* produce different quantities of β -galactosidase, the enzyme that reacts with X-gal in our assay. Batch-to-batch variation could make it difficult to correlate blue precipitate concentration with *E. coli* concentration, but the effects of this variation may be negligible. Another probable explanation for the observed batch-to-batch variation in β -galactosidase is a batch-to-batch variation in the lactose concentration in breast milk. It is well-known that the nutrients found in breast milk vary from mother to mother [71,72]. Breast milk with higher lactose expression may cause enhanced induction of the *lac* operon, which may cause enhanced expression of β -galactosidase. Further investigation is needed to determine whether additional controls or assay components are necessary to achieve consistently accurate results.

A final challenge for future teams to address is the supposed necessity of an incubator for sample testing. In the current MilkGuard protocol, milk samples should be placed under incubation at 37°C after the alginate hydrogel biosensor is added. This protocol exists because of previous work suggesting that 37°C produces the most rapid color change results [3]. However, with optimal biosensor geometry, benchtop reactions may be sufficient in low-resources settings where incubation is unavailable. Whether this is possible remains to be tested in-lab.

6.4.2 Immediate Next Steps

Immediate next steps consist of confirming the results of the geometry optimization experiment performed virtually in COMSOL Multiphysics once labs are again readily available. At this time, it will also be important that future MilkGuard teams collect more data with both cow's and human breast milk to test the accuracy of the MilkGuard algorithm and app. Observations from this data will additionally help future teams investigate the impact of batch-to-batch β -galactosidase expression discussed above.

After the app is tested with more in-lab data, it will need to be pilot tested at milk banks and improved for usability. We want the app to be usable with minimal training so that milk bank technicians can seamlessly transition to in-house bacteriological testing. Feedback from pilot testing will be crucial to achieving this goal. Related to the goal of usability, an additional immediate next-step is to determine whether or not bacterial lysis with B-PER bacterial extraction solution is necessary to reach the required lower limit of

detection. Removing this step from the MilkGuard assay (see section 4.2.1) would greatly increase the usability of our product. Given the high cost of bacterial extraction reagents, excluding bacterial lysis would also decrease the cost per sample for MilkGuard.

6.4.3 Long Term Next Steps

After the biosensor geometry and assay are optimized, the lower limit of detection is consistently reached, and batch-to-batch variabilities are addressed, future teams will need to focus on pilot testing of the MilkGuard system at breast milk banks.

Concurrently, future teams should focus on the logistics of scaling-up the manufacturing process while keeping product cost low.

Milk banks are the target customer base for the MilkGuard project. Thus, the needs of milk banks are of primary consideration at our current stage of development. That said, we envision MilkGuard becoming a product that could be marketed directly to mothers who desire to ensure the milk they are giving their infants is free of pathogens. Long term, we hope to increase the usability of MilkGuard even further so that it can be used by consumers without training.

If the model for bacteriological testing of *E. coli* presented in this paper proves to be accurate, sensitive, low-cost, and highly usable, we hope to expand the system to additional pathogens commonly found in donated human breast milk, such as strains of *Streptococcus* and *Staphylococcus*, and *Bacillus* [73]. Incorporating tests for multiple bacteriological pathogens in one system would allow milk banks to further cut production costs, further expanding infant access to optimal nutrition.

Chapter 7: Ethics and Engineering Standards

7.1 Ethical Justification

Achieving infants' equitable access to human breast milk is a worthwhile goal because of the significant potential impact that early-life breastfeeding could have on children. To lower the barrier to infants' access to breastmilk would be to promote the health and safety of infants worldwide. The MilkGuard system has the potential to make a lasting and significant impact on the availability of DHBM to infants whose mothers cannot provide breast milk. Once fully functional and distributable, MilkGuard has the potential of greatly increasing the operating efficiency at milk banks.

The MilkGuard project pushes the boundaries of biotechnology. Currently, there are no existing affordable, intuitive, and rapid diagnostic devices for DHBM. In the process, our biosensor optimization and mobile application development incorporated state-of-the-art technologies. The resulting product aims to bring about great service and benefit to our primary stakeholders—milk banks for DHBM. Other stakeholders in our project include the mothers and infants who are in need of DHBM. These are vulnerable populations who will benefit from the success of our project. With the full optimization and development of MilkGuard, we can serve milk banks, infants, and mothers in need. In this manner, the MilkGuard project encourages us to become engineers who approach our profession with competence, conscience, and compassion.

By lowering the cost of the bacterial assay of breast milk, we make the process more accessible. By developing a user-friendly smartphone application for the process, we simplify the job of milk bank technicians and thus lower the entry barrier for this position. By running computer simulation for the optimization of biosensor parameters, we pave the way for the ease of improvement of future teams. By improving on the color analysis algorithm, we improve the sensitivity and consistency of our detection method, which contributes to detecting the lower, yet still harmful levels of bacterial contamination in DHBM.

The following engineering standards delineate additional reasons for and benefits of MilkGuard.

7.2 Engineering Standards

7.2.1 Economic:

As described in section 6.3, MilkGuard offers milk banks a more affordable way to conduct bacteriological testing that is necessary for optimal infant health. In-house bacteriological testing at milk banks provides a “point-of-care” model that has the potential to reduce the cost of donated human breast milk.

7.2.2 Manufacturability

The alginate hydrogel biosensor capsules used in the MilkGuard biosensor can be easily manufactured at industrial scale. The selection of spherical alginate hydrogel geometry greatly increases the viability of mass production, as microfluidic extrusion using coaxial needles is widely used in biotechnology manufacturing. Using a mobile app for image analysis “increases” the manufacturability of our product in the sense that little manufacturing is needed for image analysis. The MilkGuard app can be widely distributed given the global prevalence of smartphones. Though this year’s MilkGuard team did not focus on the use or production of the lightbox used for smartphone image capture, we are aware that the lightbox is an additional component of the MilkGuard system that will need to be custom manufactured. Future teams could consider finding a comparable 3rd party option for image analysis to eliminate the need to contract through an additional production plant.

7.2.3 Health & safety

Literature research suggests that rigorous bacteriological testing increases the safety of donated human breast milk [3]. Thus, affordable, efficient testing methods are crucial to improving the health and safety of infants who would not otherwise have access to human breast milk. Our efforts throughout the past year have moved MilkGuard one step closer to offering milk banks a system that is affordable, efficient, *and* sensitive enough to detect HMBANA’s lower limit of detection standard of 10^4 CFU/mL [2].

7.2.4 Usability

A key consideration during the mobile app development was that it be highly usable by milk bank technicians. Using a mobile application for image analysis, rather than requiring milk banks technicians to master additional image analysis tools, decreases the duration of training required to use MilkGuard and suggests that our system may be usable in lower resource settings internationally.

7.2.5 Environmental impact

The alginate hydrogel sensor used in MilkGuard is readily biodegradable, biocompatible, and bioinert [74]. Thus, the disposal of waste produced during testing with MilkGuard should not cause environmental harm. Furthermore, the X-gal product used to detect *E. coli* via reaction with beta-galactosidase has no hazardous classifications on the Globally Harmonized System of Classification and Labelling of Chemicals [75]. However, when dissolved in dimethylformamide (DMF), X-gal powder's safety classification increases to "harmful". Since the existing MilkGuard protocol utilizes DMF, future MilkGuard teams may want to consider dissolving X-gal in a solution with a more favorable safety rating, both for the health of the environment and for the health of milk bank technicians, who are unlikely to be working in chemical safety hoods.

7.2.6 Social

The big picture goal of MilkGuard is to lower barriers to infant access to breast milk. Increasing access to donated human breast milk through low-cost bacteriological testing that can potentially be used in low-resource settings may lower infant mortality rates [76]. Though not necessarily causal, lower infant mortality rates are correlated with lower income inequality [77] and greater political gender equity [78]. While we cannot guarantee that MilkGuard will create a more socially equitable society, our efforts to make DHBM accessible to more infants are rooted in a desire to reach under-served populations.

7.2.7 Civic Engagement

In the US, the Food and Drug Administration officially recommends the use of DHBM under the direction of a physician [79]. The FDA does not directly regulate milk banks. Instead, the Human Milk Banking Association of North America (HMBANA) provides milk banks with regulatory standards [80]. Our efforts to achieve a 10^4 CFU/mL lower limit of detection requirement are based on HMBANA's official recommendations.

Chapter 8: Conclusions

Fast, affordable and accurate methods of testing breast milk for breast milk banks is crucially needed throughout the world, and the MilkGuard system was developed to address that. Previous team had achieved a low-cost biosensor that produces results in approximately four hours. Yet at the beginning of this year, MilkGuard was unable to achieve the HBMANA's lower limit of detection standard of 10^4 CFU/mL, and the assay process was difficult and unintuitive.

To reach this bacterial contamination detection level, we explored two methods: improving the MilkGuard biosensor and developing a better color analysis system.

By running COMSOL simulations while varying several parameters, we discovered the optimal geometry for MilkGuard biosensors—high volume and high surface area. Future teams would need to confirm this in physical laboratories, while keeping the manufacturing and chemical reagent costs relatively low. Our series of COMSOL simulations prove the possibility of realistically optimizing biosensors in a computer-based simulation environment, which is more economical and environmentally friendly than building hundreds of physical biosensors to test. We also developed a simulation platform that future teams can use to further improve on the MilkGuard biosensor.

By developing the MilkGuard app, we have allowed the user to easily utilize our new color analysis algorithm for the colorimetric determination of *E. coli* contamination levels. Our algorithm uses color balance, HSL conversion, and color-distance regression to improve sensitivity around the target contamination level of 10^4 CFU/mL. Future teams would need to confirm the effectiveness of our algorithm with in-lab testing, and build a more robust linear regression curve based on a larger sample size. Our improved detection sensitivity means better breastmilk testing for better infant health.

This year, our testing and developments have improved the MilkGuard system. With our developments, testing breast milk with MilkGuard is now easier and more sensitive than before. Through our simulations, we have also provided a way for future teams to improve the biosensor even more. Through our team's contribution to MilkGuard, we have striven towards infants' equitable access to breastmilk, as we try to achieve a more humane, just and sustainable world through bioengineering innovation. We look forward to when MilkGuard is fully optimized and functional as it improves infant health around the world.

Chapter 9: References

1. Newton, E.R. Breastmilk: The Gold Standard. *Clin. Obstet. Gynecol.* **2004**, *47*, 632-642.
2. Arnold, L.D. US Health Policy and Access to Banked Donor Human Milk. *Breastfeeding Medicine* **2008**, *3*, 221-229.
3. Kikuchi, N.; May, M.; Zweber, M.; Madamba, J.; Stephens, C.; Kim, U.; Mobed-Miremadi, M. Sustainable, Alginate-Based Sensor for Detection of Escherichia Coli in Human Breast Milk. *Sensors* **2020**, *20*, 1145.
4. Lactation Labs. What we Test.
5. MyMilk Mylee. MyMilk Laboratory Based Testing for Breastfeeding Pain.
6. Wu, G.; Meyyappan, M.; Lai, K.W.C. Simulation of Graphene Field-Effect Transistor Biosensors for Bacterial Detection. *Sensors* **2018**, *18*, 1715.
7. Pfeffer, C.; Liang, Y.; Grothe, H.; Wolf, B.; Brederlow, R. Towards Easy-to-use Bacteria Sensing: Modeling and Simulation of a New Environmental Impedimetric Biosensor in Fluids. *Sensors* **2021**, *21*, 1487.
8. Affi, M.; Sollicec, C.; Legentilhomme, P.; Comiti, J.; Legrand, J.; Jouanneau, S.; Thouand, G. Numerical Modeling of the Dynamic Response of a Bioluminescent Bacterial Biosensor. *Analytical and bioanalytical chemistry* **2016**, *408*, 8761-8770.
9. Moon, H.; Im, H.T.; Choi, A.; Jung, H. Real-Time Detection of Food-Borne Bacterial Adenosine Triphosphate (ATP) using Dielectrophoretic Force and a Bioluminescence Sensor. *Microchimica Acta* **2010**, *170*, 283-288.
10. Liu, J.; Jasim, I.; Shen, Z.; Zhao, L.; Dweik, M.; Zhang, S.; Almasri, M. A Microfluidic Based Biosensor for Rapid Detection of Salmonella in Food Products. *Plos one* **2019**, *14*, e0216873.
11. L. Q. Jun; G. W. bin Djaswadi; H. F. bin Hawari; M. A. B Zakariya. Simulation of Interdigitated Electrodes (IDEs) Geometry using COMSOL Multiphysics. In - 2018 International Conference on Intelligent and Advanced System (ICIAS); pp. 1-6.
12. Korzeniewska, E.; Szczęsny, A.; Lipiński, P.; Drózdź, T.; Kielbasa, P.; Miernik, A. Prototype of a Textronic Sensor Created with a Physical Vacuum Deposition Process for Staphylococcus Aureus Detection. *Sensors* **2021**, *21*, 183.
13. Wang, R.; Lum, J.; Callaway, Z.; Lin, J.; Bottje, W.; Li, Y. A Label-Free Impedance Immunosensor using Screen-Printed Interdigitated Electrodes and Magnetic Nanobeads for the

- Detection of E. Coli O157: H7. *Biosensors* **2015**, *5*, 791-803.
14. Rateni, G.; Dario, P.; Cavallo, F. Smartphone-Based Food Diagnostic Technologies: A Review. *Sensors* **2017**, *17*, 1453.
 15. Zlatev, Z. Application of a Document Camera for Color Measurement of Dairy Products.
 16. Zarei, M. Portable Biosensing Devices for Point-of-Care Diagnostics: Recent Developments and Applications. *TrAC Trends in Analytical Chemistry* **2017**, *91*, 26-41.
 17. Sununta, S.; Rattanarat, P.; Chailapakul, O.; Praphairaksit, N. Microfluidic Paper-Based Analytical Devices for Determination of Creatinine in Urine Samples. *Analytical Sciences* **2018**, *34*, 109-113.
 18. Busa, L.S.A.; Mohammadi, S.; Maeki, M.; Ishida, A.; Tani, H.; Tokeshi, M. Advances in Microfluidic Paper-Based Analytical Devices for Food and Water Analysis. *Micromachines* **2016**, *7*, 86.
 19. Zhu, H.; Sencan, I.; Wong, J.; Dimitrov, S.; Tseng, D.; Nagashima, K.; Ozcan, A. Cost-Effective and Rapid Blood Analysis on a Cell-Phone. *Lab on a Chip* **2013**, *13*, 1282-1288.
 20. Roy, M.; Jin, G.; Seo, D.; Nam, M.; Seo, S. A Simple and Low-Cost Device Performing Blood Cell Counting Based on Lens-Free Shadow Imaging Technique. *Sensors Actuators B: Chem.* **2014**, *201*, 321-328.
 21. Zhu, H.; Mavandadi, S.; Coskun, A.F.; Yaglidere, O.; Ozcan, A. Optofluidic Fluorescent Imaging Cytometry on a Cell Phone. *Anal. Chem.* **2011**, *83*, 6641-6647.
 22. D'Ambrosio, M.V.; Bakalar, M.; Bennuru, S.; Reber, C.; Skandarajah, A.; Nilsson, L.; Switz, N.; Kamgno, J.; Pion, S.; Boussinesq, M. Point-of-Care Quantification of Blood-Borne Filarial Parasites with a Mobile Phone Microscope. *Science translational medicine* **2015**, *7*, 286re4.
 23. Cesaretti, M.; Poté, N.; Dondero, F.; Cauchy, F.; Schneck, A.S.; Soubrane, O.; Paradis, V.; Diaspro, A.; Antonini, A. Testing Feasibility of an Accurate Microscopic Assessment of Macrovesicular Steatosis in Liver Allograft Biopsies by Smartphone Add-on Lenses. *Microsc. Res. Tech.* **2018**, *81*, 58-63.
 24. Kroemer, S.; Frühauf, J.; Campbell, T.M.; Massone, C.; Schwantzer, G.; Soyer, H.P.; Hofmann-Wellenhof, R. Mobile Teledermatology for Skin Tumour Screening: Diagnostic Accuracy of Clinical and Dermoscopic Image Tele-evaluation using Cellular Phones. *Br. J. Dermatol.* **2011**, *164*, 973-979.
 25. Pamplona, V.F.; Mohan, A.; Oliveira, M.M.; Raskar, R. Dual of Shack-Hartmann Optometry using Mobile Phones. In *Frontiers in Optics*; pp. FTuB4.

26. Pollock, N.R.; Rolland, J.P.; Kumar, S.; Beattie, P.D.; Jain, S.; Noubary, F.; Wong, V.L.; Pohlmann, R.A.; Ryan, U.S.; Whitesides, G.M. A Paper-Based Multiplexed Transaminase Test for Low-Cost, Point-of-Care Liver Function Testing. *Science translational medicine* **2012**, *4*, 152ra129.
27. Breslauer, D.N.; Maamari, R.N.; Switz, N.A.; Lam, W.A.; Fletcher, D.A. Mobile Phone Based Clinical Microscopy for Global Health Applications. *PloS one* **2009**, *4*, e6320.
28. Choodum, A.; Parabun, K.; Klawach, N.; Daeid, N.N.; Kanatharana, P.; Wongniramaikul, W. Real Time Quantitative Colourimetric Test for Methamphetamine Detection using Digital and Mobile Phone Technology. *Forensic Sci. Int.* **2014**, *235*, 8-13.
29. Masawat, P.; Harfield, A.; Namwong, A. An iPhone-Based Digital Image Colorimeter for Detecting Tetracycline in Milk. *Food Chem.* **2015**, *184*, 23-29.
30. Ludwig, S.K.; Zhu, H.; Phillips, S.; Shiledar, A.; Feng, S.; Tseng, D.; van Ginkel, L.A.; Nielen, M.W.; Ozcan, A. Cellphone-Based Detection Platform for rbST Biomarker Analysis in Milk Extracts using a Microsphere Fluorescence Immunoassay. *Analytical and bioanalytical chemistry* **2014**, *406*, 6857-6866.
31. Mobed-Miremadi, M.; Asi, B.; Parasseril, J.; Wong, E.; Tat, M.; Shan, Y. Comparative Diffusivity Measurements for Alginate-Based Atomized and Inkjet-Bioprinted Artificial Cells using Fluorescence Microscopy. *Artificial cells, nanomedicine, and biotechnology* **2013**, *41*, 196-201.
32. Morrison, N.; O'Connor, S.; Weber, C. MilkGuard: Low Cost Paper Sensor for the Detection of Escherichia Coli in Donated Human Breast Milk. **2017**.
33. May, M.; Kikuchi, N.; Zweber, M. MilkGuard: Low-Cost, Polymer-Based Sensor for the Detection of Escherichia Coli in Donated Human Breast Milk. **2018**.
34. Bren-Cardali, D.; Dao, L.; Destruel, J.; Fernandez, R.; Figueira, S.; Kim, U. Urinalysis Screening for Rural Communities. In 2018 IEEE Global Humanitarian Technology Conference (GHTC); pp. 1-8.
35. Brogan, E.; Haddad, A.; Woody, B. Milkguard: A Low-Cost Hydrogel Sensor for the Detection of Escherichia Coli in Donated Human Breast Milk. **2020**.
36. Gallay, C.; Girardet, A.; Viviano, M.; Catarino, R.; Benski, A.; Tran, P.L.; Ecabert, C.; Thiran, J.; Vassilakos, P.; Petignat, P. Cervical Cancer Screening in Low-Resource Settings: A Smartphone Image Application as an Alternative to Colposcopy. *International journal of women's health* **2017**, *9*, 455.
37. Raza, A.; Raza, I.; Drake, T.M.; Sadar, A.B.; Adil, M.; Baluch, F.; Qureshi, A.U.; Harrison, E.M.; Collaborative, G. The Efficiency, Accuracy and Acceptability of Smartphone-Delivered

- Data Collection in a Low-Resource Setting—a Prospective Study. *International Journal of Surgery* **2017**, *44*, 252-254.
38. Sood, M.; Chadda, R.K.; Deb, K.S.; Bhad, R.; Mahapatra, A.; Verma, R.; Mishra, A.K. Scope of Mobile Phones in Mental Health Care in Low Resource Settings. *Journal of Mobile Technology in Medicine* **2016**, *5*, 33-37.
39. Kanjo, C.; Kaasbøll, J. Mobile Technology Innovations in Low Resource Settings: A Story of Mobile Phone and Bicycle.
40. Toppo, P.; Dhote, T. PREFERENCE OF MOBILE PLATFORMS: A STUDY OF iOS VS ANDROID. *International Journal of Modern Agriculture* **2021**, *10*, 1757-1764.
41. Hansson, N.; Vidhall, T. Effects on Performance and Usability for Cross-Platform Application Development using React Native. **2016**.
42. Wu, W. React Native Vs Flutter, Cross-Platforms Mobile Application Frameworks. **2018**.
43. Novick, V. *React Native-Building Mobile Apps with JavaScript.*; Packt Publishing Ltd, 2017.
44. Expo. Introduction to Expo .
45. NPM. React-Native-Image-Colors.
46. Andriod Developers. Palette.
47. Zhao, Y.; Choi, S.Y.; Lou-Franco, J.; Nelis, J.; Zhou, H.; Cao, C.; Campbell, K.; Elliott, C.; Rafferty, K. Smartphone Modulated Colorimetric Reader with Color Subtraction. In 2019 Ieee Sensors; pp. 1-4.
48. Garud, H.; Ray, A.K.; Mahadevappa, M.; Chatterjee, J.; Mandal, S. A Fast Auto White Balance Scheme for Digital Pathology. In IEEE-EMBS International Conference on Biomedical and Health Informatics (BHI); pp. 153-156.
49. Sanila, K.H.; Balakrishnan, A.A.; Supriya, M.H. Underwater Image Enhancement using White Balance, USM and CLHE. In 2019 International Symposium on Ocean Technology (SYMPOL); pp. 106-116.
50. Ruifrok, A.C.; Johnston, D.A. Quantification of Histochemical Staining by Color Deconvolution. *Analytical and quantitative cytology and histology* **2001**, *23*, 291-299.
51. Zhang, Y.; Gao, Y.; He, Y.; Shi, Y.; Liang, K. Research on the Color Temperature & White Balance for Multimedia Sensor. *Procedia Computer Science* **2017**, *107*, 878-884.
52. Brathovde, K.; Farner, M.B.; Brun, F.K.; Sandnes, F.E. Effectiveness of Color-Picking Interfaces among Non-Designers. In International Conference on Cooperative Design,

Visualization and Engineering; pp. 181-189.

53. Thongkor, K.; Amornraksa, T. An Image Watermarking Method in HSL Color Model. In 2017 10th International Conference on Ubi-Media Computing and Workshops (Ubi-Media); pp. 1-6.

54. Saravanan, G.; Yamuna, G.; Nandhini, S. Real Time Implementation of RGB to HSV/HSI/HSL and its Reverse Color Space Models. In 2016 International Conference on Communication and Signal Processing (ICCSP); pp. 462.

55. Nishad, P.M. Various Colour Spaces and Colour Space Conversion. *Journal of global research in computer science* **2013**, *4*, 44-48.

56. Tsai, S.; Tseng, Y. A Novel Color Detection Method Based on HSL Color Space for Robotic Soccer Competition. *Comput. Math. Appl.* **2012**, *64*, 1291-1300.

57. Ehkan, P.; Siew, S.V.; Zakaria, F.F.; Warip, M.N.M.; Ilyas, M.Z. Comparative Study of Parallelism and Pipelining of RGB to HSL Colour Space Conversion Architecture on FPGA. In IOP Conference Series: Materials Science and Engineering; pp. 012054.

58. Kristianto, R.; Handayani, F.D.; Wibowo, A. Selecting the Function of Color Space Conversion RGB/HSL to Wavelength for Fluorescence Intensity Measurement on Android Based Applications. In 2019 3rd International Conference on Informatics and Computational Sciences (ICICoS); pp. 1-6.

59. Kassani, S.H.; Kassani, P.H. A Comparative Study of Deep Learning Architectures on Melanoma Detection. *Tissue and Cell* **2019**, *58*, 76-83.

60. Haase, S.; McCarthy, C.B.; Ferrelli, M.L.; Pidre, M.L.; Sciocco-Cap, A.; Romanowski, V. Development of a Recombination System for the Generation of Occlusion Positive Genetically Modified Anticarsia Gemmatalis Multiple Nucleopolyhedrovirus. *Viruses* **2015**, *7*, 1599-1612.

61. Yetisen, A.K.; Martinez-Hurtado, J.L.; Garcia-Melendrez, A.; da Cruz Vasconcellos, F.; Lowe, C.R. A Smartphone Algorithm with Inter-Phone Repeatability for the Analysis of Colorimetric Tests. *Sensors Actuators B: Chem.* **2014**, *196*, 156-160.

62. Weller, H.I.; Westneat, M.W. Quantitative Color Profiling of Digital Images with Earth Mover's Distance using the R Package Colordistance. *PeerJ* **2019**, *7*, e6398.

63. Indriani, O.R.; Kusuma, E.J.; Sari, C.A.; Rachmawanto, E.H. Tomatoes Classification using K-NN Based on GLCM and HSV Color Space. In 2017 International Conference on Innovative and Creative Information Technology (ICITech); pp. 1-6.

64. Abasi, S.; Amani Tehran, M.; Fairchild, M.D. Distance Metrics for very Large Color Differences. *Color Research & Application* **2020**, *45*, 208-223.

65. Madamba, Jerard Roniel Del Rosario. Scale Optimization of Milkguard Biosensor for Detecting E. Coli in Human Breast Milk. **2019**.
66. Kurowiak, J.; Kaczmarek-Pawelska, A.; Mackiewicz, A.G.; Bedzinski, R. Analysis of the Degradation Process of Alginate-Based Hydrogels in Artificial Urine for use as a Bioresorbable Material in the Treatment of Urethral Injuries. *Processes* **2020**, *8*, 304.
67. Landers, S.; Hartmann, B.T. Donor Human Milk Banking and the Emergence of Milk Sharing. *Pediatric Clinics* **2013**, *60*, 247-260.
68. Goldstein, L.N.; Wells, M.; Vincent-Lambert, C. The Cost-Effectiveness of Upfront Point-of-Care Testing in the Emergency Department: A Secondary Analysis of a Randomised, Controlled Trial. *Scandinavian journal of trauma, resuscitation and emergency medicine* **2019**, *27*, 1-12.
69. Rosa, L.d.S.; Mistro, S.; Oliveira, M.G.; Kochergin, C.N.; Cortes, M.L.; Medeiros, D.S.d.; Soares, D.A.; Louzado, J.A.; Silva, K.O.; Bezerra, V.M. Cost-Effectiveness of Point-of-Care A1C Tests in a Primary Care Setting. *Frontiers in Pharmacology* **2021**, *11*, 2147.
70. De Broucker, G.; Salvatore, P.P.; Mutembo, S.; Moyo, N.; Mutanga, J.N.; Thuma, P.E.; Moss, W.J.; Sutcliffe, C.G. The Cost-Effectiveness of Scaling-Up Rapid Point-of-Care Testing for Early Infant Diagnosis of HIV in Southern Zambia. *PloS one* **2021**, *16*, e0248217.
71. De Leoz, Maria Lorna A; Gaerlan, S.C.; Strum, J.S.; Dimapasoc, L.M.; Mirmiran, M.; Tancredi, D.J.; Smilowitz, J.T.; Kalanetra, K.M.; Mills, D.A.; German, J.B. Lacto-N-Tetraose, Fucosylation, and Secretor Status are Highly Variable in Human Milk Oligosaccharides from Women Delivering Preterm. *Journal of proteome research* **2012**, *11*, 4662-4672.
72. Hascoët, J.; Chauvin, M.; Pierret, C.; Skweres, S.; Van Egroo, L.; Rougé, C.; Franck, P. Impact of Maternal Nutrition and Perinatal Factors on Breast Milk Composition After Premature Delivery. *Nutrients* **2019**, *11*, 366.
73. Landers, S.; Updegrave, K. Bacteriological Screening of Donor Human Milk before and After Holder Pasteurization. *Breastfeeding Medicine* **2010**, *5*, 117-121.
74. Lee, K.Y.; Mooney, D.J. Alginate: Properties and Biomedical Applications. *Progress in polymer science* **2012**, *37*, 106-126.
75. Cayman Chemicals. X-Gal Safety Data Sheet. **2018**.
76. Israel-Ballard, K. Increasing Access and Intake of Human Milk. , **2021**.
77. Ehntholt, A.; Cook, D.M.; Rosenquist, N.A.; Muennig, P.; Pabayo, R. State-and County-Level Income Inequality and Infant Mortality in the USA in 2010: A Cohort Study. *International journal of public health* **2020**, *65*, 769-780.

78. Homan, P. Political Gender Inequality and Infant Mortality in the United States, 1990–2012. *Soc. Sci. Med.* **2017**, *182*, 127-135.
79. U.S. Food & Drug Administration. Use of Donor Human Milk . **2018**, *2021*.
80. Updegrave, K.; Festival, J.; Hackney, R.; Jones, F.; Kelly, S.; Sakamoto, P.; Vickers, A. HMBANA Standards for Donor Human Milk Banking: An Overview HMBANA Guidelines Committee. **2020**.

Chapter 10: Appendix

10.1 Team Members and Roles

Emma McCurry: Lead Contact Person, Simulation and Geometry Optimization Lead

Emma served as the lead contact person for the project, submitting various official documents and handling correspondence with Santa Clara University's School of Engineering. Before the team pivoted to a fully virtual senior design project, Emma created experimental protocols and timelines for lab-based work. After the pivot, Emma learned to use COMSOL Multiphysics and created a realistic computed-aided design simulation of the MilkGuard biosensor. Emma designed, executed, and analysed the COMSOL biosensor geometry optimization experiment.

Beau Hsia: Mobile Application and Colorimetric Algorithm Developer, Visual Design Lead

Beau served as the MilkGuard mobile application developer, coding the app from scratch (while self-learning the React Native app programming language through the process). Beau also improved upon last year's color-analysis algorithm through the addition of color balance, HSL colorspace conversion, and color-distance calculation and regression, methods he discovered through research and experimentation. Additionally, Beau designed the MilkGuard logo and colorway, which were uniformly implemented in the smartphone application and in the Senior Design Presentation package.

10.2 Key Acronyms and Abbreviations

B-PER = Bacterial Protein Extraction Reagent

CC = Microfluidic Capillary Circuit

CFU = Colony Forming Units

CFU/mL = Colony Forming Units per milliliter

COMSOL = Not an acronym, but a program title. COMSOL Multiphysics software

DHM = Donor Human Milk or Donated Human Breast Milk

DMF = Dimethylformamide

FDA= Food and Drug Administration

GHS = Globally Harmonized System of Classification and Labelling of Chemicals

HMBANA = Human Milk Banking Association of North America

HSL = Hue, Saturation, Lightness (or Luminance, or Luminosity) (Color space model)

IEEE = Institute of Electrical and Electronics Engineers

IPTG = Isopropyl β -D-1-thiogalactopyranoside

LOD = Limit of Detection

OD = Optical Density

RGB = Red, Green, Blue (Color space model)

WHO = World Health Organization

X-Gal = 5-bromo-4-chloro-3-indolyl- β -D